JPET Fast Forward. Published on September 2, 2022 as DOI: 10.1124/jpet.122.001354
This article has not been copyedited and formatted. The final version may differ from this version.

JPET-AR-2022-001354

Differential Activation and Desensitization States Promoted by Non-canonical α7 nAChR Agonists

Clare Stokes, Gisela Andrea Camacho-Hernandez[#], Ganesh A. Thakur, Xiaoxuan Wu, Palmer Taylor, and Roger L. Papke

Department of Pharmacology, Skaggs School of Pharmacy & Pharmaceutical Sciences, University of California-San Diego, La Jolla CA 92093-0751, United States (GACH, XW, PT)

Department of Pharmacology and Therapeutics, University of Florida, PO Box 100267, Gainesville FL, 32610-0267 (CS, RLP)

Department of Pharmaceutical Sciences, School of Pharmacy, Bouvé College of Health Sciences, Northeastern University, Boston, MA 02115 (GAT)

[#] current address: Medicinal Chemistry Section, Molecular Targets and Medications Discovery Branch, National Institute on Drug Abuse − Intramural Research Program, National Institutes of Health, 333 Cassell Drive, Baltimore, Maryland 21224 USA

JPET-AR-2022-001354

Running title: Non-canonical α7 nAChR Agonists

*To whom correspondence should be addressed:

Name: Roger L. Papke

Phone: 352-392-4712

Fax: 352-392-3558

E-mail: rlpapke@ufl.edu

Address: Department of Pharmacology and Therapeutics

University of Florida

P.O. Box 100267

Gainesville, FL 32610-0267

Number of text pages:.....49

Number of tables:.....3

Number of figures:.....10

Number of references:.....61

Number of words in Abstract:.....242

Number of words in Introduction: 723

Number of words in Discussion:.....1479

Abbreviations: 2NDEP, 1,1-diethyl-4(naphthalene-2-yl)piperazin-1-ium; ACh, acetylcholine; AChBP, acetylcholine binding proteins; aDPP, 2-amino dipicolyl amine pyrimidine; AR-R17779, (-)-spiro[1-azabicyclo[2.2.2]octane-3,5-oxazolidin]-2-one hydrochloride; B-973B, (S)-

3-(3,4-difluorophenyl)-N-(1-(6-(4-(pyridin-2-yl)piperazin-1-yl)- pyrazin-2-yl)ethyl)propenamide; DPP, dipicolyl pyrimidine; CAP, cholinergic anti-inflammatory pathway; CNS, central nervous system; ECD, extracellular domain; GAT-107, (3aR,4S,9bS)-4-(4-bromophenyl)-3a,4,5,9b-tetrahydro-3H-cyclopenta[c]quinoline-8sulfonamide); GTS-21, 3-(2,4-dimethoxybenzylidene)-anabaseine; nAChR, nicotinic acetylcholine receptor; MLA, methyllycaconitine; NS1738, 1-(5-chloro-2-hydroxyphenyl)-3-(2-chloro-5-(trifluoromethyl)phenyl)urea; NS6740, 1,4-diazabicyclo[3.2.2]nonan-4-yl(5-(3-(trifluoromethyl)-phenyl)-furan-2-yl)methanone; OA, orthosteric agonist; PAM, positive allosteric modulator; *p*-CF_3-diEPP, 1,1-diethyl-4-(4-(trifluoromethyl)phenyl)piperazin-1-ium iodide; PNU-120596, 1-(5-chloro-2,4-dimethoxy-phenyl)-3-(5-methyl-isoxazol-3-yl)-urea; PNU-282987, N-(3R)-1-azabicyclo[2.2.2]oct-3-yl-4-chlorobenzamidE; TMP-TQS, *cis-trans*-4-(2,3,5,6-tetramethylphenyl)-3a,4,5,9b-tetrahydro-3H-cyclopenta[c]quinoline-8-sulfonamide; TQS, 3a,4,5,9b-tetrahydro-4-(1-naphthalenyl)-3H-cyclopentan[c]quinoline-8-sulfonamide; 4BP-TQS, 4-(4-bromophenyl)-3a,4,5,9b-tetrahydro-3H-cyclopenta[c]quinoline-8-sulfonamide; WT, wild type.

Recommended section assignment: Neuropharmacology

Abstract

A series of 2,4,6-substituted pyrimidines (DPPs) were previously identified as potential α7 agonists by means of a calcium influx assay in the presence of the positive allosteric modulator (PAM) PNU-120596. The compounds lack the quaternary or strongly basic nitrogens of typical nicotinic agonists. Although differing in structure from typical nicotinic agonists, based on crystallographic data with the acetylcholine binding protein, they appeared to engage the site shared by such typical orthosteric agonists. Using oocytes expressing human α7 receptors, we found that the DPPs were efficacious activators of the receptor, with currents showing rapid desensitization characteristic of α7 receptors. However, we note that the rate of recovery from this desensitization depends strongly on structural features within the DPP family. While activation of receptors by DPP was blocked by the competitive antagonist MLA, MLA had no effect on the DPP-induced desensitization, suggesting multiple modes of DPP binding. As expected, the desensitized conformational states could be reactivated by PAMs. Mutants made insensitive to acetylcholine by the C190A mutation in the agonist binding site were weakly activated by DPPs. The observation that activation of C190A mutants by the DPP compounds was resistant to the allosteric antagonist (-)TMP-TQS supports the hypothesis that the activity of these non-canonical agonists in the orthosteric binding sites was not entirely dependent on the classical epitopes controlling activation by typical agonists and that perhaps they may access alternative modes for promoting the conformational changes associated with activation and desensitization.

Significance Statement

We report a family of nicotinic acetylcholine receptor agonists that break the rules about what the structure of an nAChR agonist should be. We show that the activity of these non-canonical agonists in the orthosteric binding sites is not dependent on the classical epitopes controlling activation by typical agonists, and that through different binding poses, they promote unique conformational changes associated with receptor activation and desensitization.

Introduction

The α7 nicotinic acetylcholine receptor (nAChR) is one of the most well-studied subtypes of a pentameric family of allosteric transmembrane proteins (Bertrand et al., 2015; Bouzat et al., 2018). It comprises five α subunits forming a homopentamer around a central cation channel, which when activated by acetylcholine (ACh) alone, has a relatively high permeability to calcium (Miller et al., 2020; Seguela et al., 1993). Each subunit contributes to two possible agonist binding faces, one at each subunit interface. Although a three-dimensional cryo-EM structure of the receptor has recently been published (Noviello et al., 2021), the degree to which the five putative orthosteric agonist (OA) binding sites contribute stoichiometrically and dynamically to activation is still unknown. Early structural data for α7, derived from mutant acetylcholine binding proteins (AChBP) (Hibbs et al., 2009), suggest that the binding sites and subunit conformations become non-equivalent as the ligands bind sequentially.

Compared to other nAChRs, α7 receptors have a low probability of opening in response to ACh, as well as a rapid desensitizing profile that is unique and known to be concentration-dependent (Papke and Lindstrom, 2020; Papke and Papke, 2002). Specifically, the level of occupation of the binding sites by agonist appears to underlie the kinetics of this desensitization, such that high levels of ACh binding appear to explicitly promote closed (i.e. desensitized) states (Papke and Lindstrom, 2020). The α7 receptors expressed in neurons have been implicated to be important for cognition, attention, regulation of aggression, and modulation of depression-like behaviors, while α7 expression in non-neuronal cells has been shown to regulate inflammation (Bagdas et al., 2018; de Jonge and Ulloa, 2007; Jones et al., 1999; Lewis et al., 2018; Mineur et al., 2018; Wang et al., 2003).

Initially, most of the efforts targeting α7 receptors were focused on orthosteric ligands and channel activation, resulting in the identification of several classes of α7-selective agonists such as AR-R17779 (Levin et al., 1999) and PNU-282987 (Bodnar et al., 2005), and partial agonists such as GTS-21 (Sullivan et al., 1995) (Figure 1A). Nonetheless, although diverse in structure, all α7-selective agonists previously identified share the structural features associated with the classic nicotinic pharmacophore (Beers and Reich, 1970), with a basic nitrogen in the core where a cationic species would prevail.

Presently, the exploration of ligands targeting α7 extends beyond the OA binding sites to extracellular allosteric activation sites that are possibly accessed via the receptor vestibule, as well as putative allosteric sites in the transmembrane domains. Various types of allosterically acting ligands are known, and include allosteric agonists like GAT107 (Figure 1A), and positive allosteric modulators (PAMs) that bind in the transmembrane domains (Young et al., 2008). Type I PAMs like NS1738 (Figure 1A) increase peak current responses to agonists, while more efficacious type II PAMs like PNU-120596 (Figure 1A) additionally convert agonist- and silent agonist-induced non-conducting (desensitized) states of receptors to active states (Hurst et al., 2005).

Employing *Lymnaea stagnalis* AChBP (Brejc et al., 2001; Camacho-Hernandez et al., 2019; Camacho-Hernandez and Taylor, 2020; Kaczanowska et al., 2017) as a structural surrogate for α7 nAChR, we identified a series of 2,4,6-substituted pyrimidine analogs (Figure 1B) that have non-canonical agonist structures, that is, they are able to activate α7 receptors selectively, but lack characteristic chemical features associated with the nicotinic pharmacophore (Beers and Reich, 1970; Sheridan et al., 1986; Tonder et al., 2001). The core structure of these compounds with partial or full agonist activity is a dipicolyl amine pyrimidine (DPP). For reading

convenience here we abbreviate the nomenclature to the substitutions on the core structure. The prefix "a" indicates an amino group in the second position of the pyrimidine core, 2-amino dipicolyl amine pyrimidine (aDPP), and the rest of the abbreviated name is related to the substitutions on the phenyl ring in position 6 of the pyrimidine ring. Initial electrophysiological characterization of these ligands (Camacho-Hernandez et al., 2019) showed activation of α7 and reduced post-application ACh-evoked responses, indicating that, to varying degrees, these DPP compounds could induce a stabilization of non-conducting or desensitized states that could be converted by application of PNU-120596 to conducting states, somewhat similarly to the silent agonist NS6740 (Briggs et al., 2009). In this article, we investigate whether the activation and desensitizing properties of the DPP compounds rely on the OA binding sites in different binding modes or whether the compounds may also be binding to allosteric sites.

Materials and Methods

Chemicals and reagents

Acetylcholine chloride (ACh) and buffer chemicals were purchased from Sigma-Aldrich (St. Louis, MO). PNU-120596 was synthesized in the laboratory of Dr. Nicole Horenstein by Dr. Kinga Chojnacka following the published procedure (Hurst et al., 2005). The 2,4,6-substituted pyrimidine analogues (DPP series) were synthesized as previously documented (Camacho-Hernandez et al., 2019; Kaczanowska et al., 2017).

Expression in Xenopus *oocytes*

The human α7 nAChR clone was obtained from Dr. J. Lindstrom (University of Pennsylvania, Philadelphia, PA). The human resistance-to-cholinesterase 3 (RIC3) clone was

obtained from Dr. M. Treinin (Hebrew University, Jerusalem, Israel) and co-injected with α7 at a ratio of 2:1 α7:RIC3 to enhance α7 receptor expression without affecting the pharmacological properties of the receptors (Halevi et al., 2003). The α7C190A mutant was made as previously described with a C116S double mutation to prevent spurious disulfide bond formation with the free cysteine (Papke et al., 2011). Subsequent to linearization and purification of the plasmid DNAs, RNAs were prepared using the mMessage mMachine in vitro RNA transcription kit (Ambion, Austin, TX). A total of 6-9 ng RNA per oocyte was injected in 50 nl water. Oocytes were maintained in Barth's solution (88 mM NaCl, 1 mM KCl, 2.38 mM $NaHCO_3$, 0.82 mM $MgSO_4$, 15 mM HEPES, 0.41 mM $CaCl_2$, 0.32 mM $Ca(NO_3)_2$, and 12 mg/l tetracycline, pH 7.6) at 16°C, and recordings were made 3-14 days after injection.

Oocytes were surgically removed from mature female *Xenopus laevis* frogs (Nasco, Ft. Atkinson, WI) as previously described (Pismataro et al., 2020). Frogs were maintained in the Animal Care Service facility of the University of Florida, and all procedures were approved by the University of Florida Institutional Animal Care and Use Committee (approval number 202002669).

Two-electrode voltage clamp electrophysiology

Experiments were conducted using OpusXpress 6000A (Molecular Devices, Union City, CA) (Papke and Stokes, 2010). Both the voltage and current electrodes were filled with 3 M KCl. Oocytes were voltage-clamped at -60 mV at room temperature (24˚C). The oocytes were bath-perfused with Ringer's solution (115 mM NaCl, 2.5 mM KCl, 1.8 mM $CaCl_2$, 10 mM HEPES, and 1 μM atropine, pH 7.2) at 2 ml/min. Control and test solutions were applied from 96-well plates via disposable tips, 400 μl at 2 ml/min. After a 30 s period of data recording to

define baseline holding currents, drug applications were 12 s in duration followed by 181 s washout periods during which time data was collected, followed by 17 s to acquire the next drug load during which time data was not recorded. Data were collected at 50 Hz and filtered at 20 Hz. The responses were calculated as both peak current amplitudes and net charge relative to the baseline, as previously described (Papke and Papke, 2002).

Data and statistical analysis

Data were analyzed by Clampfit (Molecular Devices) and Excel (Microsoft, Redmond, WA). For wild-type (WT) α7 receptors, to evaluate the experimental compounds, responses were normalized to control ACh-evoked responses, defined as the average of two initial applications of 60 μM ACh made before test applications. The average of independent 1 μM GAT107 responses were used as the controls for the α7C190A mutant receptors each day. Especially for small responses, baselines may have been manually adjusted in Clampfit to correct for rising or falling baselines in order to record the actual response accurately.

Experiments each began with eight oocytes. For WT α7 experiments, a preliminary application of control 60 μM ACh was given to assess the health and expression of each cell. An oocyte would be changed for another if it was not good. This preliminary test was not available for the α7C190A cells, which do not respond to ACh, and exposure to GAT107 affects subsequent responses. An experimental cell would be excluded from results if the two pre-control responses were inconsistent by more than 50%, if an experimental solution accidentally missed delivery, or if voltage clamp was not maintained.

Data are expressed as means ± SD from 5-8 oocytes for each experiment and plotted with Kaleidagraph 4.5.2 (Synergy Software, Reading, PA). In order to show actual data traces, means of the normalized data were calculated for each of the 10,322 points in each of the 206.44 s traces (acquired at 50 Hz), as well as the standard errors for those averages.

Net-charge responses are reported for α7 nAChR due to their concentration-dependent rapid desensitization (Papke and Papke, 2002).

Comparisons of results were made using one-way ANOVA or using t-tests between the pairs of experimental measurements. In cases where multiple comparisons were made, a Bonferroni correction for multiple comparisons (Aickin and Gensler, 1996) was applied to correct for possible false positives. A value of $p < 0.05$ was used to constitute a minimum level of significance. The statistics were calculated using an Excel template provided in Microsoft Office or ANOVA protocols in Kaleidagraph.

Results

Basic characterization of the α7 activity of the DPP compounds

The structures of the series of 2,4,6-substituted pyrimidines (DPPs) previously identified as non-canonical α7 nAChR-selective agonists are shown in Figure 1B (Camacho-Hernandez et al., 2019). All of the compounds were efficacious full or partial agonists (Supplemental Figure 1), with net-charge I_{max} values ranging from 0.64 to 1.25 compared to ACh I_{max} (Table 1) and potencies 10- to 100-fold greater than that of ACh, which has an $EC_{50} \approx 30$ μM (Papke and Papke, 2002). All nicotinic agonists promote both activation and desensitization, and the apparent efficacy of a particular compound measured with any specific experimental protocol will be affected by the balance of these processes throughout the duration of the measured

response (Papke, 2010). In the case when the induced desensitization is particularly stable, the effects of the agonist may be longer than the duration of the currents stimulated. The data indicate that, to varying degrees, the DPP compounds were very effective at inducing relatively stable inhibition/desensitization of the receptors, such that after the compounds were applied to activate the receptors, the subsequent responses to ACh were markedly decreased in a concentration-dependent manner (Figure 2A). This permitted the determination of IC_{50} values for the inhibition of the subsequent ACh controls (Camacho-Hernandez et al., 2019) (Table 1). Interestingly however, while high concentrations inhibited subsequent responses to ACh, after application at low concentrations, some of the compounds potentiated the subsequent ACh responses (Figure 2B).

The processes of activation and desensitization dynamically determine the magnitude and kinetics of these macroscopic responses, which are also strongly influenced by the drug application process itself (Papke, 2010; Papke and Papke, 2002; Quadri et al., 2018). Activation of nAChRs is always a relatively transient process compared to desensitization, and this is especially true for α7 receptors (Williams et al., 2012; Williams et al., 2011). Although the activation of α7 receptors by the DPP compounds that we can measure will always be limited by rapid onset and concomitant integrated effects of desensitization, we have several approaches available to study the nature and duration of the desensitized states produced by these compounds.

Effects of the of DPP compounds on α7 ACh-evoked responses

While the induction of the α7 desensitized states is rapid and influences the magnitude of the activation measured, the reversibility of apparent desensitization induced by the DPP

compounds can be much slower. a4H was the least potent of the compounds for producing reduction of the post-application ACh controls (Table 1), and following the application of 100 μM a4H, ACh-evoked responses returned to their original amplitude within eight minutes (Figure 3A), by the time of the second post-application ACh delivery. In contrast, there was essentially no recovery of ACh control responses after the application of 100 μM 2F4M over the course of an hour (Figure 3B). The other compounds fell between these two extremes defined by a4H and 2F4M. The Bonferroni means comparison of the responses recorded 4 minutes and 64 minutes after the DPP applications are reported in Table 2. The data for these recoveries could be fit to an exponential function to define time constants (τ) for recovery, either based on the fit of the averaged data or of the individual replicates (Supplemental Figures 2-8 and Table 3). The ANOVA on the time constants of replicate data (Figure 3C) is provided in the Supplemental Data.

Differing effects of methyllycaconitine on 2F4M activation and desensitization

We tested whether the α7-selective competitive antagonist methyllycaconitine (MLA) (Alkondon, 1992) would block activation by 2F4M and, by doing so, prevent the induction of long-lived inhibition/desensitization produced by this compound. Since the α7 agonist-evoked responses occur during the leading edge of the drug applications (Papke and Papke, 2002), we first preapplied 100 μM MLA for 30 s before co-applying 100 μM MLA and 10 μM 2F4M. While MLA effectively blocked the 2F4M activation, the inhibition/desensitization of subsequent ACh-evoked responses was indistinguishable from that observed when 10 μM 2F4M was applied alone (Figure 4). This suggests that the activation and desensitization produced by

2F4M may arise from different binding modes, one MLA-sensitive and the other MLA-insensitive, respectively.

PAM-sensitive desensitization induced by DPP compounds

Of all nAChR, α7 receptors have the lowest probability of opening and normally open for extremely brief periods of time, if at all, before entering into desensitized states (Williams et al., 2011). The extent to which the responses of α7 receptors are regulated by desensitization (Papke and Lindstrom, 2020; Uteshev et al., 2002) has been revealed by the effects of type II PAMs like PNU-120596, which can reactivate previously desensitized receptors and promote bursts of currents lasting many seconds (Andersen et al., 2016; Williams et al., 2011). The use of type II PAMs have also shown that specific ligands can induce extremely stable desensitized states, still detectable an hour or longer after drug application (Pismataro et al., 2021). In order to test the hypothesis that the DPP compounds that produced long-lasting inhibition of ACh responses did so by inducing stable desensitization that was in part PAM-sensitive, we applied the compounds at 30 μM and, without further applications of ACh, washed the cells for 30 minutes before applying 10 μM PNU-120596 alone (Figure 5A). The concentration of 30 μM was chosen because it was approximately the IC_{50} for a4H the least potent compound for residual inhibition (Table 1), and 30 minutes a good separation of predicted recoveries, based on Figure 3B. All compounds that effectively reduced ACh responses (*i.e.* all but a4H) primed the receptors to respond to the delayed application of the PAM (Figure 5B, see Supplemental Data for ANOVA results). The log magnitude of the delayed PNU-120596 responses was well correlated to the amount of residual inhibition (Figure 5C, R = 0.985).

TMP-TQS sensitivity of 2F4M-primed activation by PNU-120596

To test the hypothesis that 2F4M may bind to a previously identified allosteric activation site of α7 receptors, we determined whether (-)TMP-TQS (Gill et al., 2012; Papke et al., 2020), an antagonist of the allosteric agonist GAT107 (the active isomer of 4BP-TQS) (Gill et al., 2011; Thakur et al., 2013), would be able to block the 2F4M-primed responses to delayed applications of PNU-120596. As shown in Figure 6, co-application of 100 μM of (-)TMP-TQS totally blocked responses to an application of PNU-120596 primed by the earlier application of 10 μM 2F4M. However, this inhibition was transient and did not perturb the desensitization induced by the initial application of 2F4M since cells treated with (-)TMP-TQS were as sensitive to a second PNU-120596 application as cells that received just two applications of the PAM (see Supplemental Data for ANOVA results). This indicates that the prolonged effects of 2F4M were not perturbed by this antagonist binding to an allosteric site. These results are consistent with 2F4M binding either in a unique manner to the orthosteric sites or to other unidentified sites to produce long-term desensitization.

Activity of DPP compounds on C190A mutants

We have previously characterized the C190A α7 mutant as being non-orthosterically activatible due to its insensitivity to ACh (Gulsevin et al., 2019). However, considering that the test compounds are so structurally divergent from ACh and other typical agonists, we examined the activity of specific DPP compounds on the C190A mutant, utilizing a range of concentrations higher than required for activation of WT α7 receptors. When applied at sufficiently high concentrations, 2F4M could activate α7C190A receptors; although without PAM co-applications, the magnitudes of the responses were relatively small compared to the 1 μM

GAT107 control responses, with peak currents typically less than 1 μA (Figure 7). To test whether 2F4M was working at the allosteric site to activate and desensitize C190A receptors, we co-applied 2F4M and varying concentrations of (-)TMP-TQS (Papke et al., 2020) to α7C190A (Figure 7A). Either 100 or 300 μM 2F4M was applied alone or co-applied with 30, 100, or 300 μM (-)TMP-TQS. The (-)TMP-TQS applications were entirely ineffective at reducing either the direct activation of the C190A mutant (Figure 7A and 7C left) or the priming of the receptors to subsequent application of 10 μM PNU-120596 alone (Figure 7B and 7C right). Note that this lack of (-)TMP-TQS effect during the 2F4M application is in great contrast with the effects of (-)TMP-TQS when co-applied with the PNU-120596 following 2F4M priming (Figure 7D).

The observation that the 2F4M-induced desensitization persisted when 2F4M was co-applied with the allosteric antagonist indicates that the desensitization induced by 2F4M, and detected with the PNU-120596 applications, was not likely due to 2F4M binding to the allosteric site targeted by (-)TMP-TQS.

Dynamics of response potentiation and recovery from desensitization.

We investigated whether there were dynamic interactions between PAM-mediated activation of 2F4M-desensitized receptors and the recovery of ACh sensitivity. We sought to determine if recovery was strictly time dependent or could be accelerated by episodes of PAM-potentiated activation. We induced a less-than-total level of desensitization with a single application of 30 μM 2F4M, which permitted partial recovery of ACh responses over the course of an hour (Figure 8A). We made alternating applications of 60 μM ACh and 10 μM PNU-120596 at four-minute intervals (Figures 8B & 8C). While the single application of 30 μM 2F4M reduced ACh responses for over an hour (Figure 8A), repeated applications of PNU-

120596 promoted the recovery of ACh responses after the single 30 μM application (Figure 8B). Note that to keep the ACh responses in register between the two experiments, only every other ACh response is shown in Figure 8A. When the ACh responses were alternated with PNU-120596 applications, the net charge of the ACh responses became nearly three times the original values (Figure 8C). For the PAM to have these augmented effects, it is likely that it was retained at least to some degree at the transmembrane binding site or otherwise remained available to rebind. There is also evidence for persistent effects of 2F4M at its binding site since applications of PNU-120596 alone continued to produce activation that was not statistically different from the initial PNU responses (Supplemental Figure 9). The switch from reduced to the enhanced ACh responses (Figure 8C) suggests that the PNU-120596 applications either allowed orthosteric sites to become available for binding ACh or restored the ability of ACh binding to promote channel activation.

Repeated PNU-120596 effects on ACh responses in the absence of 2F4M desensitization

When applied alone, PNU-120596 fails to activate α7 receptors, and in general its effects as a potentiator are transient and only apparent when applied to previously desensitized receptors or when co-applied with an agonist. However, we observed in a control experiment (Figure 9A) that when PNU-120596 was applied repeatedly in a protocol similar to that illustrated in Figure 8B, but without the desensitizing effects of 2F4M, there was a progressive increase in ACh control responses (Figure 9B). It may be the case that PNU-120596 accumulated at sites on the receptor, in the chamber itself, or partitioned into the oocyte membrane as nicotine can (Jia et al., 2003). It is interesting though, that effects on ACh responses by the repeated PNU-120596 applications paralleled the increased ACh responses in the experiment with 2F4M, although

beginning from a different baseline (Figure 9C). The potentiating effects of alternating applications of 10 μM PNU-120596 were essentially the same when the PNU-120596 was co-applied with 30 μM (-)TMP-TQS (Supplemental Figure 10). It is interesting to note that there were proportionately greater increases in net charge compared to peak currents. Although this was more apparent after 2F4M (Figure 9D), the differences were not significant.

Discussion

State functions for the nAChR in muscle were initially defined by Katz and Thesleff in 1957, when they described recovery from desensitization as slow, whereas dissociation of the ligand was more rapid (Katz and Thesleff, 1957). Studies of direct pharmacological relevance came to light in the muscle nicotinic receptor by Rang and Ritter, who demonstrated that desensitization would be extended to other ligands by defining metaphilic antagonists that not only blocked the receptor but promoted desensitization (Rang and Ritter, 1970a; Rang and Ritter, 1970b). Subsequently, Sine and Taylor were able to show that local anesthetics enhanced the affinity of orthosteric agents (Sine and Taylor, 1979) and that in the muscle receptor there were two defined sites, presumably at the alpha subunit interfaces, that promoted agonist responses, and occupation of only one of the two sites was necessary for competitive antagonism by snake toxins (Sine and Taylor, 1980; Sine and Taylor, 1981). The extension of these concepts to the α7 receptor might have been expected to yield structural simplification in employing a homomeric pentamer for structural studies; however, each monomer in the pentamer may experience local conformational freedom, resulting in a certain amount of structural stochasticity. That is, based on ligand binding, intersubunit interactions, or thermodynamic flexibility, each monomer within a pentamer may adopt more than one conformation, resulting in

a certain amount of structure variability within the population of receptors. Indeed, we have shown through molecular dynamic studies that the pentamer does not maintain a five-fold axis of symmetry while interacting with ligands (Gulsevin et al., 2020; Gulsevin et al., 2019). These considerations notwithstanding, more complexity enters the equation since addition of ligands in a polynomial fashion creates additional asymmetry at the binding site interfaces, heterogeneous stoichiometry of site occupation, and unresolved questions of possible subunit cooperativity.

Although lacking the typical features of nAChR agonists, the substituted pyrimidine compounds appear to function as α7-selective agents, hypothetically by binding in unique ways to the subunit interfaces associated with the binding sites for more typical orthosteric agonists. Camacho-Hernandez and Taylor demonstrated that the 2-dipicolyl amine substitution at the 4-position in the pyrimidine core is crucial for agonism and that the substitution in the 6-position is important to modulate this agonism (Camacho-Hernandez et al., 2019). Hence this family of congeneric compounds can serve as agonists and antagonists and promote transitions among at least three states: activatable closed channels, active open channels, and desensitized non-functional channels. The molecular and structural determinants of the varying desensitization produced by the DPP compounds remains to be resolved, although in general the aDPP compounds were less desensitizing than the DPP compounds, suggesting that the 2-amino moiety plays a role either by direct interaction and/or by affecting the pK_a of the pyrimidine ring.

It is difficult to define an analog of the classic pharmacophore for a nicotinic agonist within the structures of the DPP compounds. This raises the questions of not only the stoichiometry but the pose of these compounds when bound to the nAChR. This is particularly so for the DPP series since a cationic center is integral to virtually all orthosteric agonists associating with the α7 nAChR, but the pK_as of the pyrimidine and pyridine nitrogens are low in

the DPP series, making it likely that the nitrogens are unprotonated to varying degree at physiologic pH (Camacho-Hernandez et al., 2019). These considerations led us to speculate that the DPP compounds might be influenced by, or working through, allosteric sites of α7 to produce activation and/or desensitization rather than strictly through the OA sites common to nAChR and the AChBP.

A hypothetical model for α7 state transitions with progressive levels of ACh binding is shown in Figure 10A. As ligands bind, it is likely that the symmetry and equivalence of the ligand binding sites change, with some sites adopting higher affinity for agonists, associated with desensitized forms of the receptor. Additional factors may influence the state transitions regulated by the binding of DPP compounds like 2F4M, consistent with the differential effects of MLA on activation and desensitization. The binding mode associated with activation may be only a low-affinity interaction within the traditional binding pocket, since activation is seen as a transient process for all of the DPP compounds. However, the desensitizing effects may come from associations with an as yet undefined binding pocket, and for some of the DPP compounds this may represent a higher affinity binding, consistent with the stability of the desensitization produced by agents like 2F4M. In the absence of PAM-dependent activation, these binding actions may remain stable and prevent ACh from binding or at least from producing activation. The condition at the end of the sequence of alternating applications of 2F4M and PNU-120596 (Figure 8C) seems paradoxical since the recovery of sensitivity to ACh might suggest a relief of desensitization, while the persistent activity of PNU-120596 applied alone suggests that the receptors remain desensitized. A likely resolution of this apparent paradox is suggested by the character of the ACh responses obtained at the end of the sequence of applications (Figure 9D). The ACh responses do not resemble those of receptors in the normal resting state but rather those

of receptors that have been allosterically potentiated by residual/accumulating PAM, so in effect they are consistent with PAM-dependent activation of desensitized receptors.

Shown in Figure 10B is a proposed model for PNU-120596 activation of α7 at different levels of agonist occupancy (adopted from (Papke and Horenstein, 2021)). Our data suggest that the high-affinity binding of 2F4M, which is stabilized in a desensitized conformation, may be modified as a consequence of the conformational changes associated with PAM-dependent destabilization of the desensitized state, so that the repeated presentations of PNU-120596 alter the nature of the 2F4M-induced desensitization. It may be that the ligand slips out of the high-affinity binding site that is created during the desensitization process and that as the receptor "breathes" (fluctuates among activated and desensitized states), the ligand can dissociate, or the receptor otherwise relax, making some of the sites available to bind ACh or alternatively allowing ACh binding to be more effectively coupled to channel activation via the effects of the accumulating PAM. Under these conditions, the ACh activity is not typical since it clearly benefits from, and likely depends on, the residual PNU-120596 activity, as was seen in the control experiment (Figure 9B). The results of PNU-120596 selectively promoting greater net-charge responses suggests that there are fundamental effects on the α7 activation processes, yet without relieving the desensitization required for PNU-120596 to activate the receptors when applied alone.

Initially we considered the hypothesis that the prolonged desensitization profile of the DPP compounds might be due to interactions at allosteric sites, which was encouraged by the unique structural features departing from traditional orthosteric agonists. However, the observation that TMP-TQS produced only transient block of PAM priming by 2F4M with the WT receptors suggested that the prolonged 2F4M-induced desensitization was not a result of a

direct interaction with the allosteric site targeted by TMP-TQS but rather due to an alternative mode of binding at sites related to orthosteric activation. Binding of DPP compounds to the α7 receptor apparently breaks some of the rules associated with the canonical nAChR agonist pharmacophore, consistent with their ability to activate ACh-insensitive C190A receptors.

The identification of the role played by α7 in the cholinergic anti-inflammatory pathway (CAP) (Bagdas et al., 2018; Tracey, 2007) has indicated that α7 has both ionotropic and metabotropic properties and suggested that channel activation may not be critical for the anti-inflammatory profile of ligands targeting α7 (Thomsen and Mikkelsen, 2012). This in turn led to the discovery of silent agonists such as NS6740 (Figure 1A) as potential therapeutics for inflammation.

In some ways, the activity profile of 2F4M resembles that of the strongly desensitizing partial agonist NS6740, which is an effective activator of CAP (Papke et al., 2015) but is actually an antagonist of the procognitive effects of other more efficacious α7 agonists such as A-582941 (Briggs et al., 2009) and BMS-902483 (Pieschl et al., 2017). The basis for the effectiveness of NS6740, and possibly DPP compounds like 2F4M, in CAP is that the non-conducting states associated with ion-channel desensitization may, in fact, be signal-transducing states that mediate G-Protein function (King et al., 2017) or other intracellular second-messenger pathways (Kabbani and Nichols, 2018; King et al., 2018). Therefore, it will be of immediate interest to determine the pharmacokinetic profiles of the DPP compounds, such as metabolic stability, blood brain barrier penetration and whether they are effective as α7 drugs in vivo.

In conclusion, the family of DPP compounds are a major structural departure and an opportunity to investigate a potentially important paradigm shift in the development of nAChR pharmacology. Our nascent understanding of their function as α7 activators and desensitizers

challenges many of our current models, and reconsideration of those models is likely to lead to new insights and further exploration of alternative models.

Acknowledgments

Oocyte recordings were conducted by Lu Wenchi Corrie.

Authorship Contributions

Participated in research design: GACH, PT, RLP, CS

Conducted experiments: CS

Contributed new reagents or analytic tools: GACH, XW, PT, GAT

Performed data analysis: CS, RLP

Wrote or contributed to the writing of the manuscript: GACH, PT, CS, RLP

References

Aickin M and Gensler H (1996) Adjusting for multiple testing when reporting research results: the Bonferroni vs Holm methods. *American journal of public health* **86**(5): 726-728.

Alkondon M, Pereira, E.F.R., Wonnacott, S., and Albuquerque, E.X. (1992) Blockade of nicotinic currents in hippocampal neurons defines methyllycaconitine as a potent and specific receptor antagonist. *Mol Pharmacol* **41**: 802-808.

Andersen ND, Nielsen BE, Corradi J, Tolosa MF, Feuerbach D, Arias HR and Bouzat C (2016) Exploring the positive allosteric modulation of human alpha7 nicotinic receptors from a single-channel perspective. *Neuropharmacology* **107**: 189-200.

Bagdas D, Gurun MS, Flood P, Papke RL and Damaj MI (2018) New Insights on Neuronal Nicotinic Acetylcholine Receptors as Targets for Pain and Inflammation: A Focus on alpha7 nAChRs. *Curr Neuropharmacol* **16**(4): 415-425.

Beers WH and Reich E (1970) Structure and activity of acetylcholine. *Nature* **228**: 917-922.

Bertrand D, Lee CH, Flood D, Marger F and Donnelly-Roberts D (2015) Therapeutic Potential of alpha7 Nicotinic Acetylcholine Receptors. *Pharmacol Rev* **67**(4): 1025-1073.

Bodnar AL, Cortes-Burgos LA, Cook KK, Dinh DM, Groppi VE, Hajos M, Higdon NR, Hoffmann WE, Hurst RS, Myers JK, Rogers BN, Wall TM, Wolfe ML and Wong E (2005) Discovery and structure-activity relationship of quinuclidine benzamides as agonists of alpha7 nicotinic acetylcholine receptors. *J Med Chem* **48**(4): 905-908.

Bouzat C, Lasala M, Nielsen BE, Corradi J and Esandi MDC (2018) Molecular function of alpha7 nicotinic receptors as drug targets. *J Physiol* **596**(10): 1847-1861.

Brejc K, van Dijk WJ, Klaassen RV, Schuurmans M, van Der Oost J, Smit AB and Sixma TK (2001) Crystal structure of an ACh-binding protein reveals the ligand-binding domain of nicotinic receptors. *Nature* **411**(6835): 269-276.

Briggs CA, Gronlien JH, Curzon P, Timmermann DB, Ween H, Thorin-Hagene K, Kerr P, Anderson DJ, Malysz J, Dyhring T, Olsen GM, Peters D, Bunnelle WH and Gopalakrishnan M (2009) Role of channel activation in cognitive enhancement mediated by alpha7 nicotinic acetylcholine receptors. *Br J Pharmacol* **158**(6): 1486-1494.

Camacho-Hernandez GA, Stokes C, Duggan BM, Kaczanowska K, Brandao-Araiza S, Doan L, Papke RL and Taylor P (2019) Synthesis, Pharmacological Characterization, and Structure-Activity Relationships of Noncanonical Selective Agonists for alpha7 nAChRs. *J Med Chem* **62**(22): 10376-10390.

Camacho-Hernandez GA and Taylor P (2020) Lessons from nature: Structural studies and drug design driven by a homologous surrogate from invertebrates, AChBP. *Neuropharmacology*: 108108.

de Jonge WJ and Ulloa L (2007) The alpha7 nicotinic acetylcholine receptor as a pharmacological target for inflammation. *Br J Pharmacol* **151**(7): 915-929.

Gill JK, Dhankher P, Sheppard TD, Sher E and Millar NS (2012) A series of alpha7 nicotinic acetylcholine receptor allosteric modulators with close chemical similarity but diverse pharmacological properties. *Mol Pharmacol* **81**(5): 710-718.

Gill JK, Savolainen M, Young GT, Zwart R, Sher E and Millar NS (2011) Agonist activation of {alpha}7 nicotinic acetylcholine receptors via an allosteric transmembrane site. *Proc Natl Acad Sci U S A* **108**(14): 5867-5872.

Gulsevin A, Papke RL and Horenstein N (2020) In silico modeling of the alpha7 nicotinic acetylcholine receptor: new pharmacological challenges associated with multiple modes of signaling. *Mini Rev Med Chem*.

Gulsevin A, Papke RL, Stokes C, Garai S, Thakur GA, Quadri M and Horenstein N (2019) Allosteric agonism of alpha7 nicotinic acetylcholine receptors. *Mol Pharmacol* **95**(6): 604-614.

Halevi S, Yassin L, Eshel M, Sala F, Sala S, Criado M and Treinin M (2003) Conservation within the RIC-3 gene family. Effectors of mammalian nicotinic acetylcholine receptor expression. *J Biol Chem* **278**(36): 34411-34417.

Hibbs RE, Sulzenbacher G, Shi J, Talley TT, Conrod S, Kem WR, Taylor P, Marchot P and Bourne Y (2009) Structural determinants for interaction of partial agonists with acetylcholine binding protein and neuronal alpha7 nicotinic acetylcholine receptor. *EMBO J* **28**(19): 3040-3051.

Hurst RS, Hajos M, Raggenbass M, Wall TM, Higdon NR, Lawson JA, Rutherford-Root KL, Berkenpas MB, Hoffmann WE, Piotrowski DW, Groppi VE, Allaman G, Ogier R, Bertrand S, Bertrand D and Arneric SP (2005) A novel positive allosteric modulator of the alpha7 neuronal nicotinic acetylcholine receptor: in vitro and in vivo characterization. *J Neurosci* **25**(17): 4396-4405.

Jia L, Flotildes K, Li M and Cohen BN (2003) Nicotine trapping causes the persistent desensitization of alpha4beta2 nicotinic receptors expressed in oocytes. *J Neurochem* **84**(4): 753-766.

Jones S, Sudweeks S and Yakel JL (1999) Nicotinic receptors in the brain: correlating physiology with function. *Trends Neurosci* **22**(12): 555-561.

Kabbani N and Nichols RA (2018) Beyond the Channel: Metabotropic Signaling by Nicotinic Receptors. *Trends Pharmacol Sci* **39**(4): 354-366.

Kaczanowska K, Camacho Hernandez GA, Bendiks L, Kohs L, Cornejo-Bravo JM, Harel M, Finn MG and Taylor P (2017) Substituted 2-Aminopyrimidines Selective for alpha7-Nicotinic Acetylcholine Receptor Activation and Association with Acetylcholine Binding Proteins. *J Am Chem Soc* **139**(10): 3676-3684.

Katz B and Thesleff S (1957) A study of the "desensitization" produced by acetylcholine at the motor end-plate. *Journal of Physiology (London)* **138**: 63-80.

King JR, Gillevet TC and Kabbani N (2017) A G protein-coupled alpha7 nicotinic receptor regulates signaling and TNF-alpha release in microglia. *FEBS Open Bio* **7**(9): 1350-1361.

King JR, Ullah A, Bak E, Jafri MS and Kabbani N (2018) Ionotropic and Metabotropic Mechanisms of Allosteric Modulation of alpha7 Nicotinic Receptor Intracellular Calcium. *Mol Pharmacol* **93**(6): 601-611.

Levin ED, Bettegowda C, Blosser J and Gordon J (1999) AR-R17779, and alpha7 nicotinic agonist, improves learning and memory in rats. *Behavioural pharmacology* **10**(6-7): 675-680.

Lewis AS, Pittenger ST, Mineur YS, Stout D, Smith PH and Picciotto MR (2018) Bidirectional Regulation of Aggression in Mice by Hippocampal Alpha-7 Nicotinic Acetylcholine Receptors. *Neuropsychopharmacology* **43**(6): 1267-1275.

Miller DR, Khoshbouei H, Garai S, Cantwell LN, Stokes C, Thakur G and Papke RL (2020) Allosterically Potentiated alpha7 Nicotinic Acetylcholine Receptors: Reduced Calcium Permeability and Current-Independent Control of Intracellular Calcium. *Molecular Pharmacology* **98**(6): 695-709.

Mineur YS, Mose TN, Blakeman S and Picciotto MR (2018) Hippocampal alpha7 nicotinic ACh receptors contribute to modulation of depression-like behaviour in C57BL/6J mice. *Br J Pharmacol* **175**(11): 1903-1914.

Noviello CM, Gharpure A, Mukhtasimova N, Cabuco R, Baxter L, Borek D, Sine SM and Hibbs RE (2021) Structure and gating mechanism of the alpha7 nicotinic acetylcholine receptor. *Cell*.

Papke RL (2010) Tricks of Perspective: Insights and limitations to the study of macroscopic currents for the analysis of nAChR activation and desensitization. *Journal of Molecular Neuroscience* **40**(1-2): 77-86.

Papke RL, Bagdas D, Kulkarni AR, Gould T, AlSharari S, Thakur GA and Damaj IM (2015) The analgesic-like properties of the alpha7 nAChR silent agonist NS6740 is associated with nonconducting conformations of the receptor. *NeuroPharm* **91**: 34-42.

Papke RL, Garai S, Stokes C, Horenstein NA, Zimmerman AD, Abboud KA and Thakur GA (2020) Differing Activity Profiles of the Stereoisomers of 2,3,5,6TMP-TQS, a Putative Silent Allosteric Modulator of alpha7 nAChR. *Mol Pharmacol* **98**(4): 292-302.

Papke RL and Horenstein NA (2021) Therapeutic targeting of alpha7 nicotinic acetylcholine receptors. *Pharm Reviews* **73**(3): 1118-1149.

Papke RL and Lindstrom JM (2020) Nicotinic acetylcholine receptors: Conventional and unconventional ligands and signaling. *Neuropharmacology* **168**: 108021.

Papke RL and Papke JKP (2002) Comparative pharmacology of rat and human alpha7 nAChR conducted with net charge analysis. *Br J of Pharm* **137**(1): 49-61.

Papke RL and Stokes C (2010) Working with OpusXpress: methods for high volume oocyte experiments. *Methods* **51**(1): 121-133.

Papke RL, Stokes C, Williams DK, Wang J and Horenstein NA (2011) Cysteine accessibility analysis of the human alpha7 nicotinic acetylcholine receptor ligand-binding domain identifies L119 as a gatekeeper. *Neuropharmacology* **60**(1): 159-171.

Pieschl RL, Miller R, Jones KM, Post-Munson DJ, Chen P, Newberry K, Benitex Y, Molski T, Morgan D, McDonald IM, Macor JE, Olson RE, Asaka Y, Digavalli S, Easton A, Herrington J, Westphal RS, Lodge NJ, Zaczek R, Bristow LJ and Li YW (2017) Effects of BMS-902483, an alpha7 nicotinic acetylcholine receptor partial agonist, on cognition and sensory gating in relation to receptor occupancy in rodents. *Eur J Pharmacol* **807**: 1-11.

Pismataro MC, Horenstein NA, Stokes C, Dallanoce C, Thakur GA and Papke RL (2021) Stable desensitization of alpha7 nicotinic acetylcholine receptors by NS6740 requires interaction with S36 in the orthosteric agonist binding site. *Eur J Pharmacol* **905**: 174179.

Pismataro MC, Horenstein NA, Stokes C, Quadri M, De Amici M, Papke RL and Dallanoce C (2020) Design, synthesis, and electrophysiological evaluation of NS6740 derivatives: Exploration of the structure-activity relationship for alpha7 nicotinic acetylcholine receptor silent activation. *Eur J Med Chem* **205**: 112669.

Quadri M, Bagdas D, Toma W, Stokes C, Horenstein NA, Damaj MI and Papke RL (2018) The antinociceptive and anti-inflammatory properties of the alpha7 nAChR weak partial agonist p-CF3N,N-diethyl-N'-phenylpiperazine. *J Pharmacol Exp Ther* **367**(2): 203-214.

Rang HP and Ritter JM (1970a) On the mechanism of desensitization at cholinergic receptors. *Mol Pharmacol* **6**(4): 357-382.

Rang HP and Ritter JM (1970b) The relationship between desensitization and the metaphilic effect at cholinergic receptors. *Mol Pharmacol* **6**(4): 383-390.

Seguela P, Wadiche J, Dinely-Miller K, Dani JA and Patrick JW (1993) Molecular cloning, functional properties and distribution of rat brain alpha 7: a nicotinic cation channel highly permeable to calcium. *J Neurosci* **13(2)**: 596-604.

Sheridan RP, Nilakantan R, Dixon JS and Venkataraghavan R (1986) The ensemble approach to distance geometry: application to the nicotinic pharmacophore. *J Med Chem* **29**(6): 899-906.

Sine S and Taylor P (1979) Functional consequences of agonist-mediated state transitions in the cholinergic receptor. Studies in cultured muscle cells. *J Biol Chem* **254**: 3315-3325.

Sine S and Taylor P (1980) The relationship between agonist occupation and the permeability response of the cholinergic receptor revealed by bound cobra alpha-toxin. *J Biol Chem* **255**: 10144-10156.

Sine SM and Taylor P (1981) Relationship between reversible antagonist occupancy and the functional capacity of the acetylcholine receptor. *J Biol Chem* **256**: 6692-6699.

Sullivan JP, Decker MW, Donnelly-Roberts D, Brioni JD, Bannon AW, Holladay MW, Anderson DJ, Briggs CA, Williams M and Arneric SP (1995) Cholinergic channel activators: novel opportunities for the treatment of CNS disorders. *Proc West Pharmacol Soc* **38**: 127-130.

Thakur GA, Kulkarni AR, Deschamps JR and Papke RL (2013) Expeditious Synthesis, Enantiomeric Resolution and Enantiomer Functional Characterization of (4-(4-bromophenyl)-3a,4,5,9b-tetrahydro-3H-cyclopenta[c]quinoline-8-sulfonamide (4BP-TQS) an Allosteric agonist –Positive Allosteric Modulator of alpha7 nAChR. *Journal of Medicinal Chemistry* **56**: 8943-8947.

Thomsen MS and Mikkelsen JD (2012) The alpha7 nicotinic acetylcholine receptor ligands methyllycaconitine, NS6740 and GTS-21 reduce lipopolysaccharide-induced TNF-alpha release from microglia. *J Neuroimmunol* **251**(1-2): 65-72.

Tonder JE, Olesen PH, Hansen JB, Begtrup M and Pettersson I (2001) An improved nicotinic pharmacophore and a stereoselective CoMFA-model for nicotinic agonists acting at the central nicotinic acetylcholine receptors labelled by. *Journal of computer-aided molecular design* **15**(3): 247-258.

Tracey KJ (2007) Physiology and immunology of the cholinergic antiinflammatory pathway. *The Journal of clinical investigation* **117**(2): 289-296.

Uteshev VV, Meyer EM and Papke RL (2002) Activation and inhibition of native neuronal alpha-bungarotoxin-sensitive nicotinic ACh receptors. *Brain Res* **948**(1-2): 33-46.

Wang H, Yu M, Ochani M, Amella CA, Tanovic M, Susarla S, Li JH, Yang H, Ulloa L, Al-Abed Y, Czura CJ and Tracey KJ (2003) Nicotinic acetylcholine receptor alpha7 subunit is an essential regulator of inflammation. *Nature* **421**(6921): 384-388.

Williams DK, Peng C, Kimbrell MR and Papke RL (2012) The Intrinsically Low Open Probability of alpha7 nAChR Can be Overcome by Positive Allosteric Modulation and Serum Factors Leading to the Generation of Excitotoxic Currents at Physiological Temperatures. *Mol Pharmacol* **82**(4): 746-759.

Williams DK, Wang J and Papke RL (2011) Investigation of the Molecular Mechanism of the Alpha7 nAChR Positive Allosteric Modulator PNU-120596 Provides Evidence for Two Distinct Desensitized States. *Mol Pharmacol* **80**(6): 1013-1032.

Young GT, Zwart R, Walker AS, Sher E and Millar NS (2008) Potentiation of alpha7 nicotinic acetylcholine receptors via an allosteric transmembrane site. *Proc Natl Acad Sci U S A* **105**(38): 14686-14691.

This research was supported by the National Institutes of Health Grants, GM57481, EY024717, and GM18360

No author has an actual or perceived conflict of interest with the contents of this article.

Figure Legends

Figure 1. Compounds relevant to these studies. **A)** Previously characterized compounds. **B)** aDPP and DPP compounds used in these experiments.

Figure 2. Enhancement and inhibition of post-application ACh responses by DPP compounds. **A)** Follow-up net-charge responses of α7 receptors to 60 μM ACh 4 minutes after single 12-second applications of the DPP compounds (Methods) at the indicated concentrations. Each point is the average (± SD) of 5-8 cells, normalized to the average of two initial ACh control responses obtained from the same cells. Data were fit to the Hill equation assuming a negative slope and allowing the initial I_{max} to be fit as an experimental parameter (Table 1). **B)** Statistical comparisons of the initial controls and the ACh responses following the application the DPP compounds at a concentration of 300 nM. Significant increases in the ACh responses were noted for four of the compounds (*$p < 0.05$, ** $p < 0.0001$, corrected for multiple comparisons). Full ANOVA provided in Supplemental Data.

Figure 3. Varying recovery of ACh controls on oocytes expressing human α7 nAChR following application of 100 μM DPP and aDPP compounds. **A)** Averaged raw data for ACh responses prior to and following 100 μM application of representative DPP compounds. Data for individual cells (n = 8, 5, and 8, for a4H, a2M, and 2F4M, respectively) were normalized to the ACh peak current amplitudes from the same cells prior to the DPP applications. Data on averaged response (dark line) and SEM (tan shaded areas) were calculated for each of 10,322 points over the 206.44-second acquisition periods. **B)** Average net-charge values (± SD, n = 5-8

cells) of repeated ACh applications following 100 μM DPP applications recorded at 4-minute intervals over the course of an hour. The averaged data were fit to an equation for exponential recovery of the response (R_t) from a baseline (base), representing the extrapolated inhibition/desensitization immediately after the DPP application and a time constant (τ) for recovery back to original control response amplitude: $R_t = base + (1 - e^{-t/\tau})$. Fit values and correlation coefficients are provided in Table 3. Also provided in Table 3 are the averaged fits (± SD) of the single-cell replicates (Supplemental Figures 2-8). **C)** Dot plots of fitted time constants for each replicate cell of each compound.

Figure 4. MLA effects on 2F4M activation and desensitization of α7. After recording two initial ACh control responses, cells were treated with 100 μM MLA 30 s without washout from the chamber prior to standard application of 100 μM MLA alone or co-applied with 10 μM 2F4M. Subsequently eleven further applications of 60 μM ACh were made to evaluate recovery from MLA inhibition and/or 2F4M-induced desensitization/inhibition. For comparison, other cells were treated with 10 μM 2F4M without MLA and evaluated for their subsequent ACh responses. As shown to the left, the MLA treatment (purple diamonds) eliminated 2F4M activation observed when the drug was applied alone (black diamonds). The inhibition of ACh responses following treatment with MLA alone fully reversed through the course of the experiment (red circles), while the desensitization/inhibition produced by 2F4M was essentially identical for cells with (purple circles) or without MLA co-application (black circles). All points are the average net-charge responses (± SD) of 8 cells. ANOVA (see Supplemental Data) indicated that following MLA, the ACh responses were greater in cells receiving MLA alone

than cells receiving 2F4M and MLA ($p < 0.001$) and that there were no significant differences at any time point between the two 2F4M groups.

Figure 5. Decreased controls correspond to increased sensitivity to PNU-120596 applied alone to α7-expressing cells. **A)** Averaged raw data (see Methods) for the three of the DPP compounds shown in Figure 3 indicating initial ACh controls, the responses to 30 μM DPP applications, and after a 30-minute wash the responses to 10 μM PNU-120596 alone (n = 8, 6, and 7 for a4H, a2M, and 2F4M, respectively). **B)** Dot plots showing each net-charge response of α7-expressing cells (n = 6-8, ± SEM) to 10 μM PNU applications 30 minutes after 30 μM DPP and aDPP compound applications, normalized to the initial ACh controls. Black bars indicate the means. **C)** Scatter plot of the PNU-120596 responses shown in panel B to the residual inhibition after 30 minutes (data taken from Figure 3B). Residual inhibition was calculated as 1 minus the response at the 30-minute time point in 3B. The fit function was Inhibition = 0.544 + 0.203 Log (PNU-120596 response), R = 0.9825. Note that the left-most point is quite distant from the others, so we also evaluated the fit if that point was omitted. In that case the fit function was, Inhibition = 0.503 + 0.240 Log (PNU-120596 response), R = 0.908. This alternative fit is represented by the red line in the plot.

Figure 6. TMP-TQS inhibition of 2F4M-primed responses of α7 nAChR to PNU-120596. **A)** Averaged net-charge responses (black lines) of six cells (± SEM, shaded areas) to control applications of 60 μM ACh, followed by 10 μM 2F4M, a subsequent application of 60 μM ACh, and then two applications of 10 μM PNU-120596, at four minute intervals. The upper traces (n = 5) are from cells receiving PNU-120596 alone on the last two applications. The cells

represented in the lower traces (n = 6) received 100 μM of the most active (-) isomer of TMP-TQS during the first application of PNU-120596. **B)** Dot plots of the averaged net-charge data (± SEM) from the cells in A (ANOVA information available in the Supplemental Data).

Figure 7. Effects of co-applications of TMP-TQS on responses of C190A α7 mutants. Data are normalized to the average responses to 1 μM GAT107 on the same day from the same batch of injected oocytes. **A)** Dot plots with means indicated for net-charge responses to 2F4M applications of 100 or 300 μM alone or with increasing concentration of (-)TMP-TQS. The only significant effect of TMP-TQS co-application ($p < 0.05$, see Supplemental Data for ANOVA) was a small increase in the 300 μM response. **B)** Responses to 10 μM PNU-120596 applied alone 4 minutes after panel A responses. Data are the net-charge responses of 5-8 oocytes, normalized to the average responses of α7C190A-expressing cells to 1 μM GAT107 obtained on the same day with cells from the same injection set. Note the differences in scale between panels A and B, reflecting the small size and transient nature of the responses to 2F4M applied alone. **C)** The averaged raw data traces (n = 6) for the responses to 300 μM 2F4M, applied alone or co-applied with 300 μM (-)TMP-TQS. Traces on the left are the responses to the initial 2F4M application. Traces on the right are the responses to 10 μM PNU-120596 applied four minutes after the initial 2F4M applications. Black lines indicate the mean response to 2F4M alone, with tan SEM, and blue lines show the mean response to 2F4M co-applied with (-)TMP-TQS, with aqua SEM. **D)** The effects of (-)TMP-TQS co-application with PNU-120596 on α7C190A responses primed by a prior application of 300 μM 2F4M. The group of traces on the left shown the averaged raw data (n = 5, ± SEM) for applications of 300 μM 2F4M applied alone followed up with applications of 10 μM PNU-120596, alone or co-applied with 300 (-)TMP-TQS. On the

right are shown a superimposition of the PNU-120596 responses, illustrating the significant effect of (-)TMP-TQS when co-applied ($p < 0.01$).

Figure 8. Effect of repeated PNU-120596 applications on ACh recoveries of α7-expressing cells. **A)** The inhibition and slow recovery of ACh responses after 30 μM 2F4M. All responses were reduced compared to the initial ACh responses (black asterisks, ANOVA with Dunnett's Multiple Comparisons), and the last two ACh responses are increased compared to the first post-application response (red asterisks). Note that only every other ACh response in the complete sequence is shown, to be in register with the data in panel C. **B)** The averaged raw data from cells treated alternately with ACh and 10 μM PNU-120596 after a single application of 30 μM 2F4M ($n = 6$). Prior to averaging, the raw data were normalized based on the peak of the ACh control obtained from the same cells. **C)** Net-charge responses to the ACh and 2F4M applications in the sequence of response illustrated in panel B. Compared to the initial ACh controls (ANOVA with Dunnett's Multiple Comparisons), the first two ACh applications were significantly reduced (black asterisks). However, with repeated applications of PNU-120596, responses increased, and the last three applications in the sequence were larger than the initial controls (red asterisks). Note that the size of the PNU-120596 responses in this experiment did not change significantly in this experiment (Supplemental Figure 9).

Figure 9. Effects of control experiment PNU-120596 applications on 60 μM ACh responses of α7-expressing cells. **A)** The averaged raw data from a control experiment with alternating applications of 60 μM ACh and 10 μM PNU-120596. **B)** The sequence of ACh net-charge responses compared to the initial ACh controls. Significant increases, compared to the ACh

prior to the first PNU-120596 application (red circles) are indicated by red asterisks (ANOVA with Dunnett's Multiple Comparisons, see Supplemental Data). **C)** Comparison of ACh increases due to alternating PNU-120596 applications under control conditions in panel B (blue circles) and following initial inhibition by 30 μM 2F4M (red circles, data taken from Figure 8C). Plotted are the averages ± S.D from the data in the dot plots. **D)** Averaged raw data comparisons of initial controls (black lines with tan representing the SEM) and ACh responses after augmentation by alternating applications of 10 μM PNU-120596. The upper traces are from the experiment shown in panels A and B with the final ACh response in dark and light blue. The lower traces are the from the experiment illustrated in Figure 8, with the average final ACh response in red and the SEM in pink.

Figure 10. Models. **A)** Hypothetical effects of increasing effects of receptor binding to ACh (upper scheme) or 2F4M (lower scheme), representing changes in binding sites and channel gating. ACh binding is assumed to be more rapidly reversible than 2F4M binding. **B)** Hypothetical energy landscapes of state transitions as functions of agonist occupancy and PNU-120596 binding (adapted from (Papke and Horenstein, 2021)). If 2F4M can dissociate more rapidly from the PNU-120596-activated channels than from receptors not bound by PNU-120596, then repeated bouts of PNU-120596 activation might free up sites for ACh binding and activation.

Table 1. Net-charge activity of test compounds on WT α7 receptors.

	Response I_{max}*	**EC_{50}, μM***	**Recovery I_{max}**	**IC_{50}, μM**
a4H	0.64 ± 0.03	0.37 ± 0.08	1.22 ± 0.11	39.91 ± 20.05
a2F4M	0.78 ± 0.04	0.11 ± 0.03	1.20 ± 0.12	0.42 ± 0.17
2M	0.78 ± 0.02	2.98 ± 0.32	1.61 ± 0.21	2.95 ± 1.35
2F4M	0.72 ± 0.07	0.67 ± 0.27	1.59 ±0.40	1.04 ± 0.82
2F	0.99 ± 0.03	2.55 ± 3.96†	1.35 ± 0.14	4.47 ± 1.54
a4M	0.77 ± 0.03	0.92 ± 0.12	2.27 ± 0.31	1.85 ± 1.08
a2M	1.25 ± 0.36	1.35 ± 0.39	2.20 ± 0.21	0.50 ± 0.18

I_{max} is normalized to ACh I_{max}, and I_{max} of post-control responses are normalized to 60 μM ACh pre-control responses.

*See Supplemental Figure 1.

†These data were not well fit by the Hill Equation, so that while the Imax value is a reasonable indication of efficacy, the EC50 value has an unsatisfactory error range.

Table 2. Data for the Bonferroni means comparison of data in Figure 3

2.1 Significant differences between responses to ACh at t = 4 minutes*

Comparison	difference	q	p	95% confidence interval
a4H vs 2F4M	0.779	16.89	< .0001	0.577 to 0.981
a4H vs a2M	0.774	15.229	< .0001	0.551 to 0.997
a4H vs 2M	0.771	17.309	< .0001	0.576 to 0.967
a4H vs 2F	0.769	16.679	< .0001	0.567 to 0.971
a4H vs a4M	0.766	15.899	< .0001	0.554 to 0.976
a4H vs a2F4M	0.764	16.567	< .0001	0.562 to 0.967

* All other pairwise comparisons were not significantly different

2.2 Significant differences between responses to ACh at t = 64 minutes*

Comparison	difference	q	p	95% confidence interval
a4H vs 2F4M	1.180	9.933	< .0001	0.659 to 1.700
a4H vs 2F	1.033	8.695	< .0001	0.5122 to 1.553
a4H vs a4M	0.859	6.928	< .001	0.316 to 1.402
a4H vs 2M	0.858	7.480	< .0001	0.355 to 1.361
a4H vs a2F4M	0.829	6.9799	< .0001	0.308 to 1.350

* All other pairwise comparisons were not significantly different

JPET Fast Forward. Published on September 2, 2022 as DOI: 10.1124/jpet.122.001354
This article has not been copyedited and formatted. The final version may differ from this version.

Table 3. Recovery from DPP inhibition/desensitization

	Values from replicates					Values from fits in Figure 3B				
Drug	τ, s	SD	base	SD	n	τ, s	error	base	error	r
a4H	47.65	35.84	0.62	0.20	7	19.19	2.53	0.40	0.03	0.984
a2F4M	146.34	111.60	-0.03	0.04	7	110.15	6.59	-0.01	0.01	0.9862
2M	111.03	53.78	-0.05	0.07	7	91.54	9.54	-0.04	0.03	0.967
2F4M	1952.09	1512.73	-0.03	0.07	8	1410.50	150.01	0.04	0.03	0.902
2F	319.23	1320	-0.01	0.06	7	224.85	17.81	-0.01	0.01	0.967
a4M	776.93	1097.07	-0.07	0.05	6	51.78	4.47	-0.08	0.03	0.989
a2M	53.18	39.59	-0.06	0.07	5	98.59	5.25	-0.03	0.01	0.990

A

Reference compounds

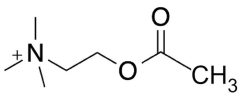

Acetylcholine

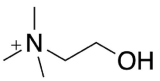

Choline

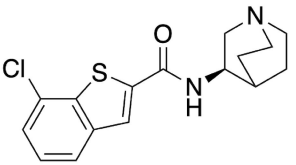

Encenicline

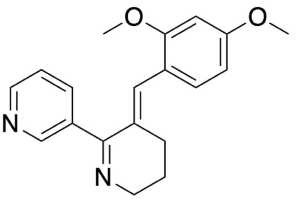

GTS-21

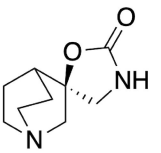

AR-R17779

Agonists

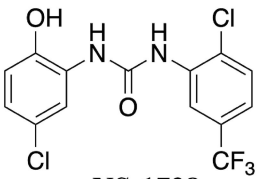

NS-1738

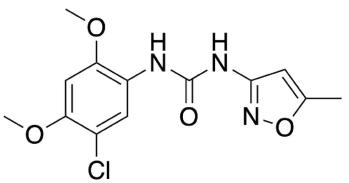

PNU-120596

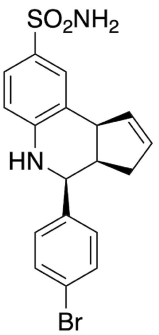

GAT-107

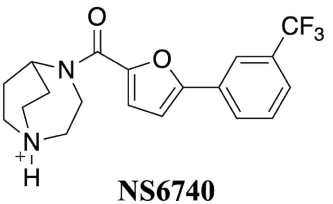

NS6740

PAM Type I **PAM Type II** **Ago-PAM** **Silent Agonist**

B

aDPP Compounds

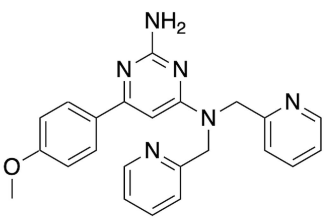

a4M

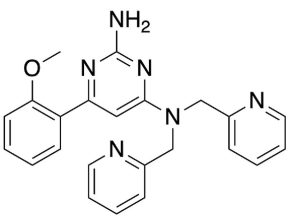

a2M

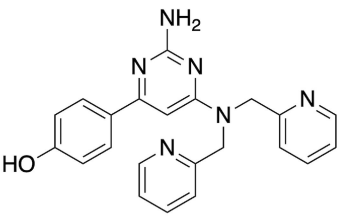

a4H

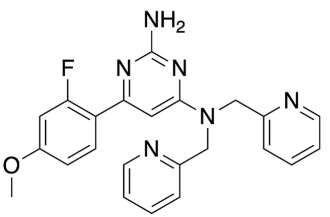

a2F4M

DPP Compounds

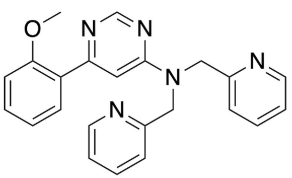

2M

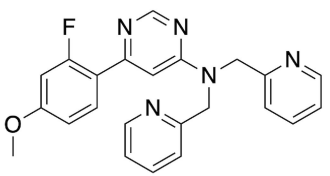

2F4M

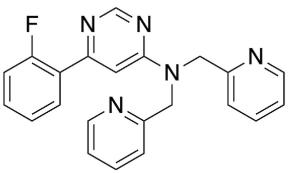

2F

Non Canonical agonists

Figure 1

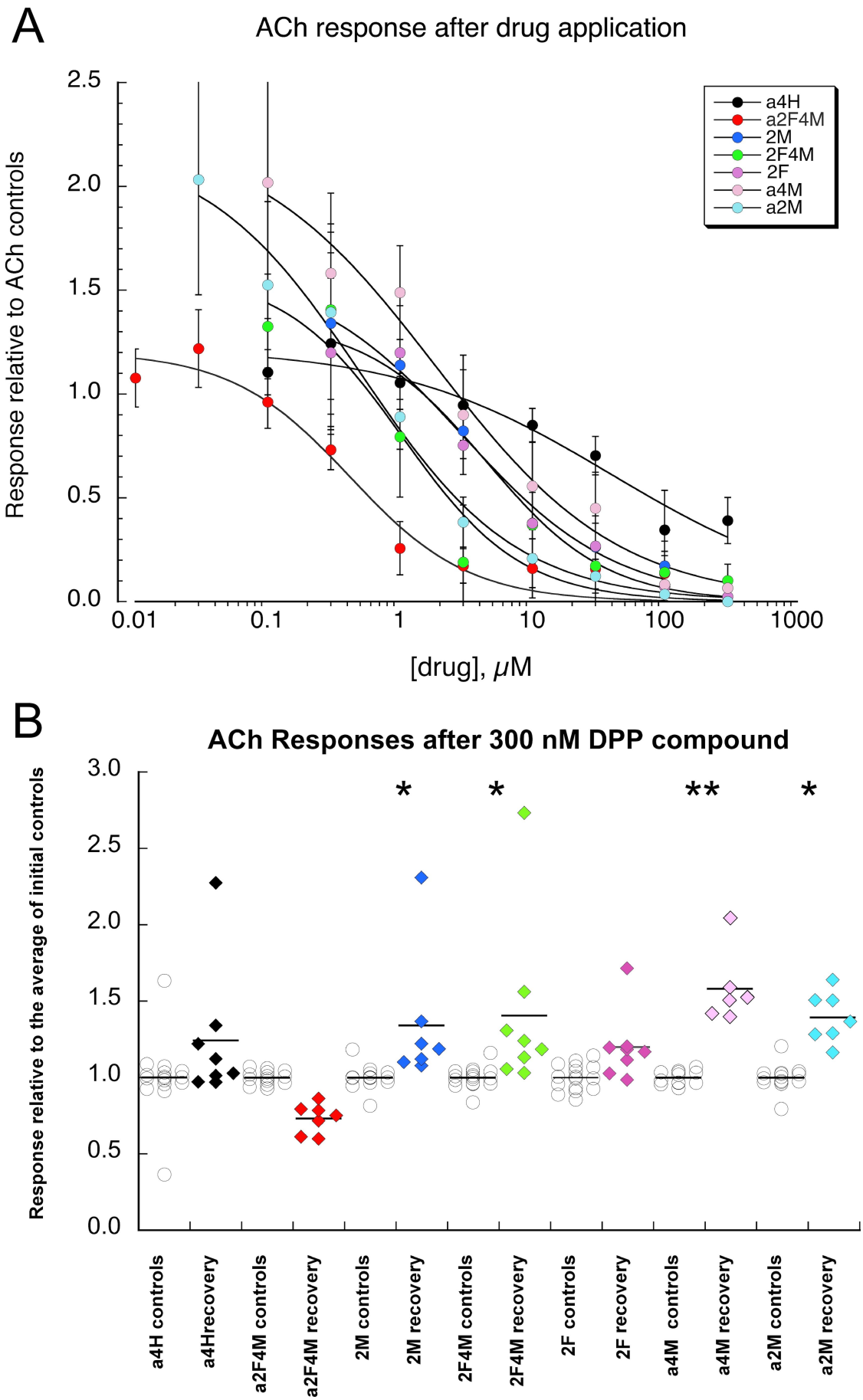
A
ACh response after drug application
Response relative to ACh controls
[drug], μM
a4H
a2F4M
2M
2F4M
2F
a4M
a2M
B
ACh Responses after 300 nM DPP compound
Response relative to the average of initial controls
a4H controls
a4Hrecovery
a2F4M controls
a2F4M recovery
2M controls
2M recovery
2F4M controls
2F4M recovery
2F controls
2F recovery
a4M controls
a4M recovery
a2M controls
a2M recovery

Figure 2

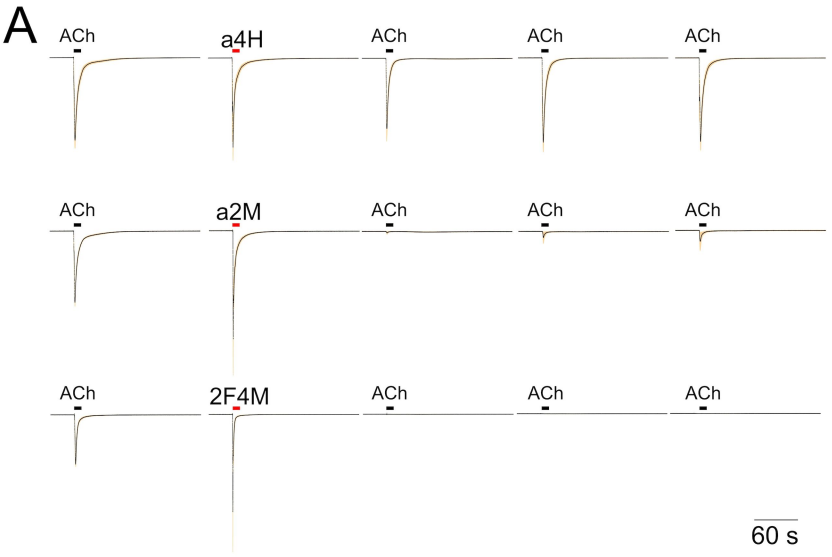
A
ACh
a4H
ACh
ACh
ACh
ACh
a2M
ACh
ACh
ACh
ACh
2F4M
ACh
ACh
ACh
60 s

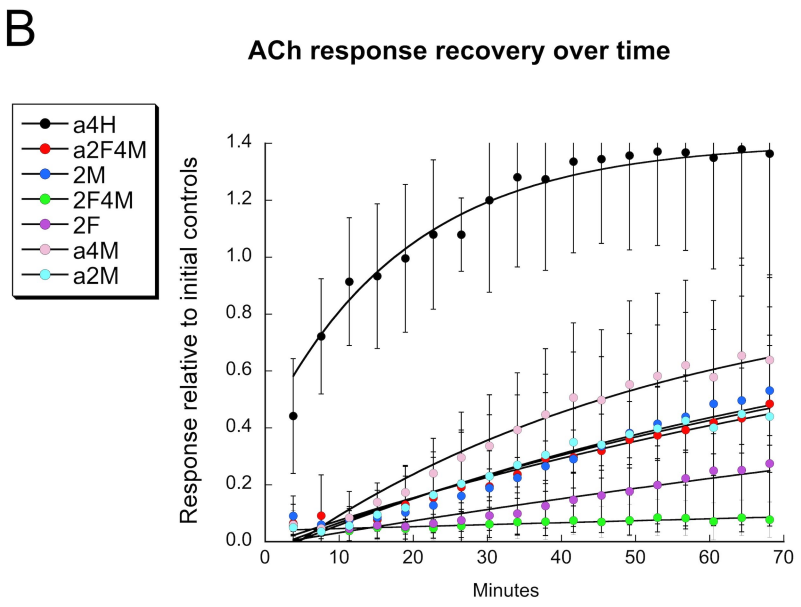
B
ACh response recovery over time
a4H
a2F4M
2M
2F4M
2F
a4M
a2M
Response relative to initial controls
1.4
1.2
1.0
0.8
0.6
0.4
0.2
0.0
0
10
20
30
40
50
60
70
Minutes

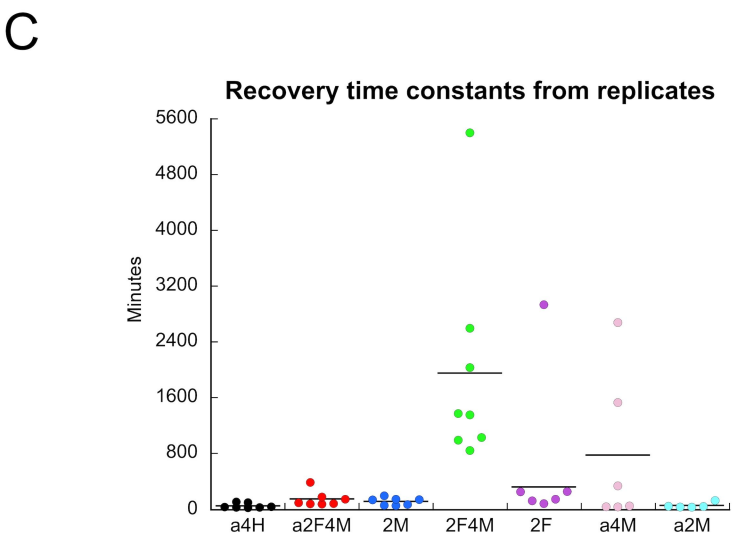
C
Recovery time constants from replicates
Minutes
5600
4800
4000
3200
2400
1600
800
0
a4H
a2F4M
2M
2F4M
2F
a4M
a2M

Figure 3

Recovery of ACh responses, effects of 10 μM 2F4M and MLA

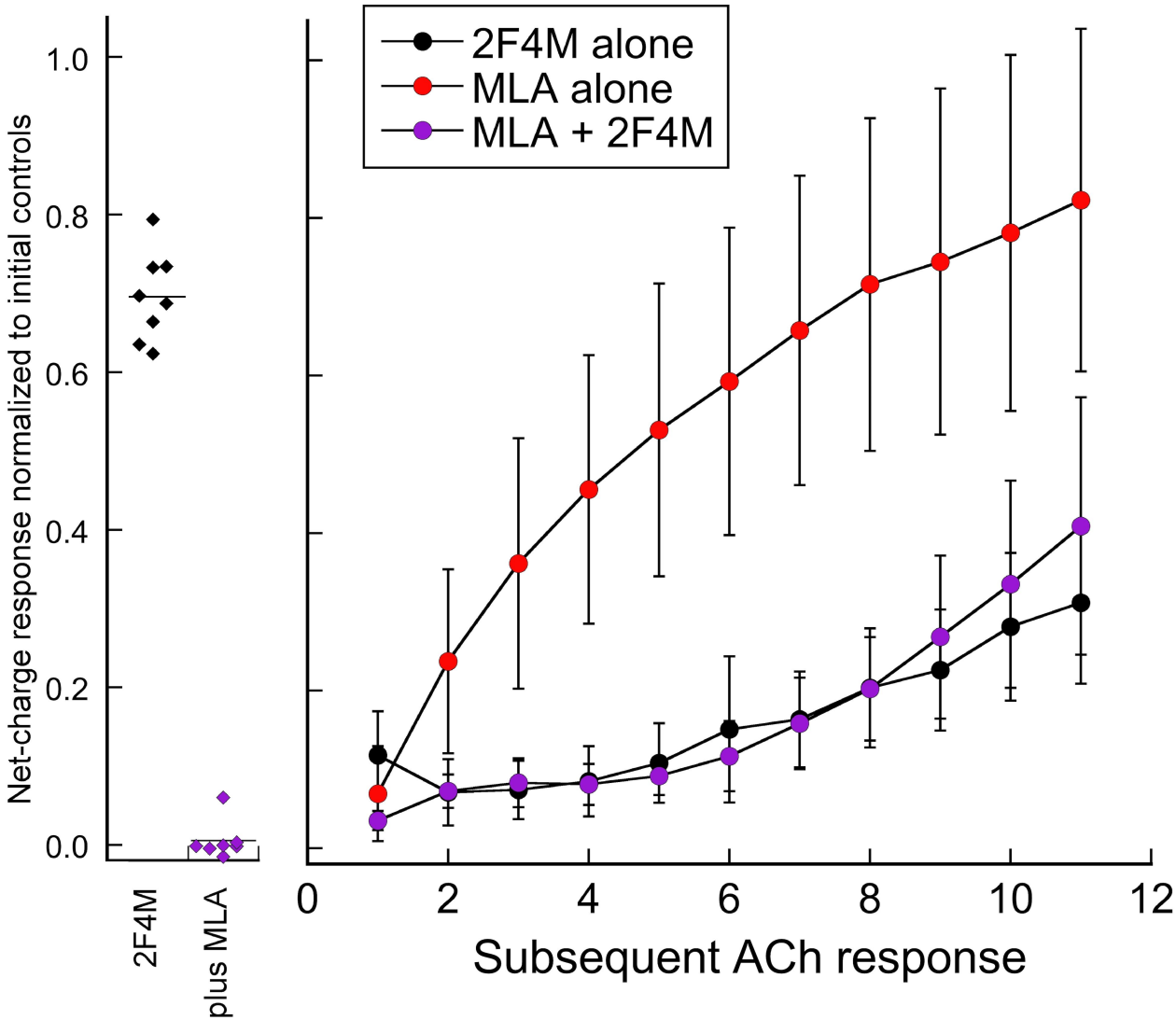

Figure 4

Responses of wild-type α7 to 10 μM PNU-120596 30 minutes after 30 μM DPP

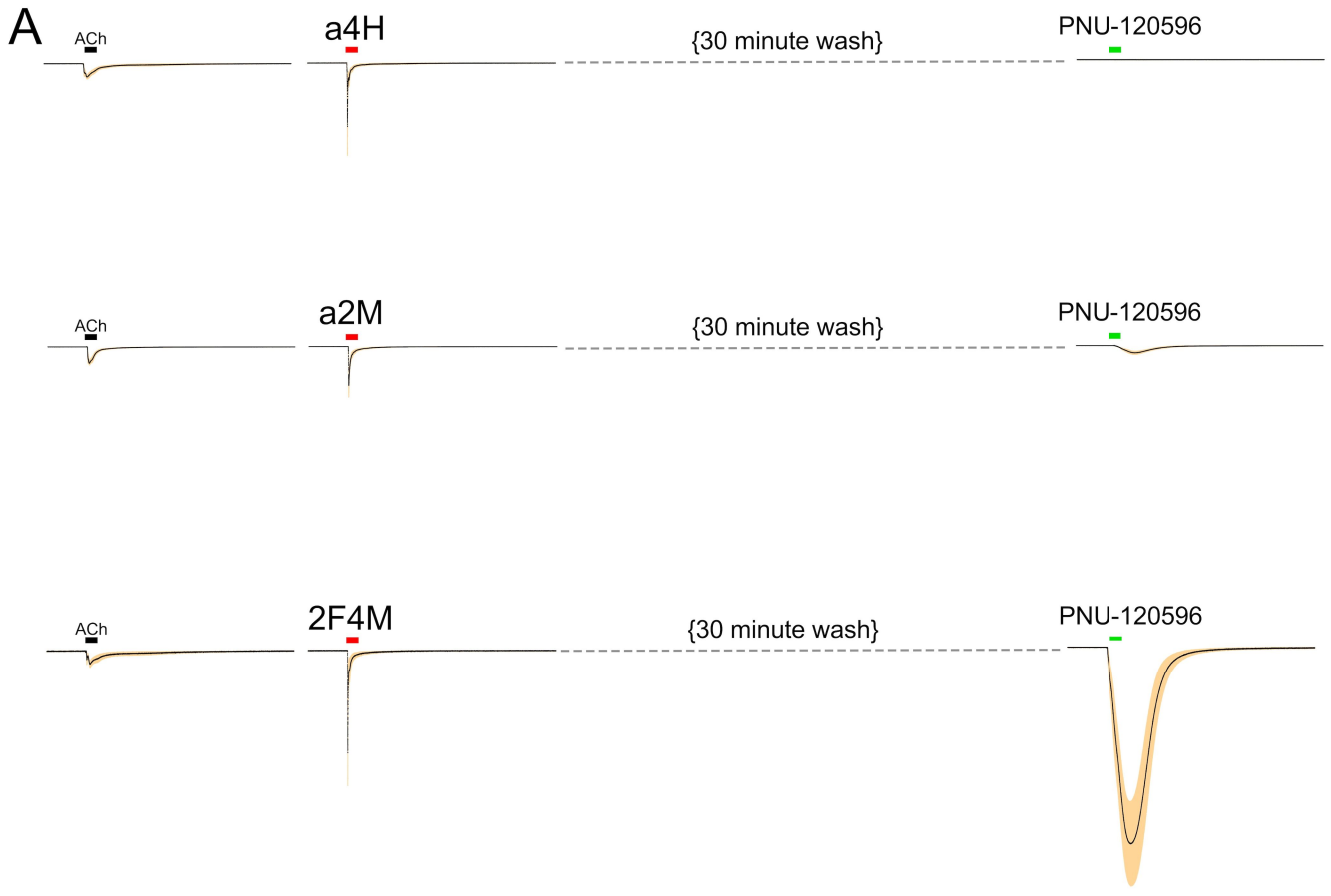

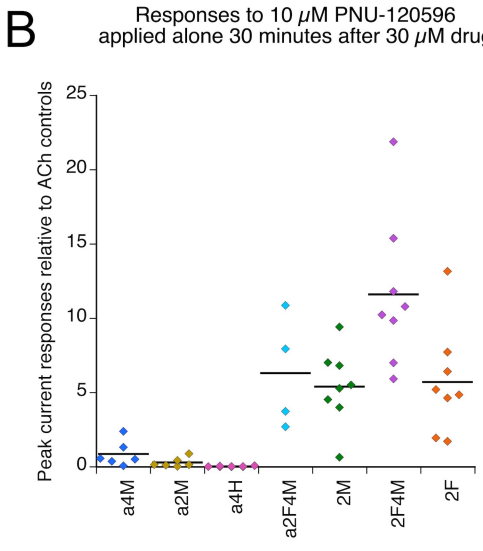

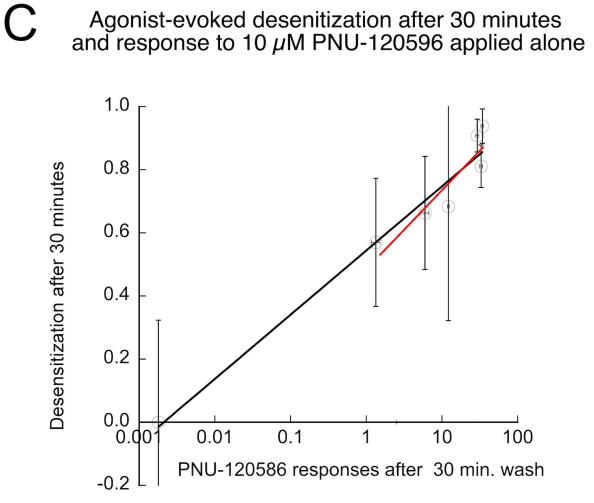

Figure 5

A

Effect of (-)TMP-TQS on 2F4M-primed responses to PNU-120596 applied alone

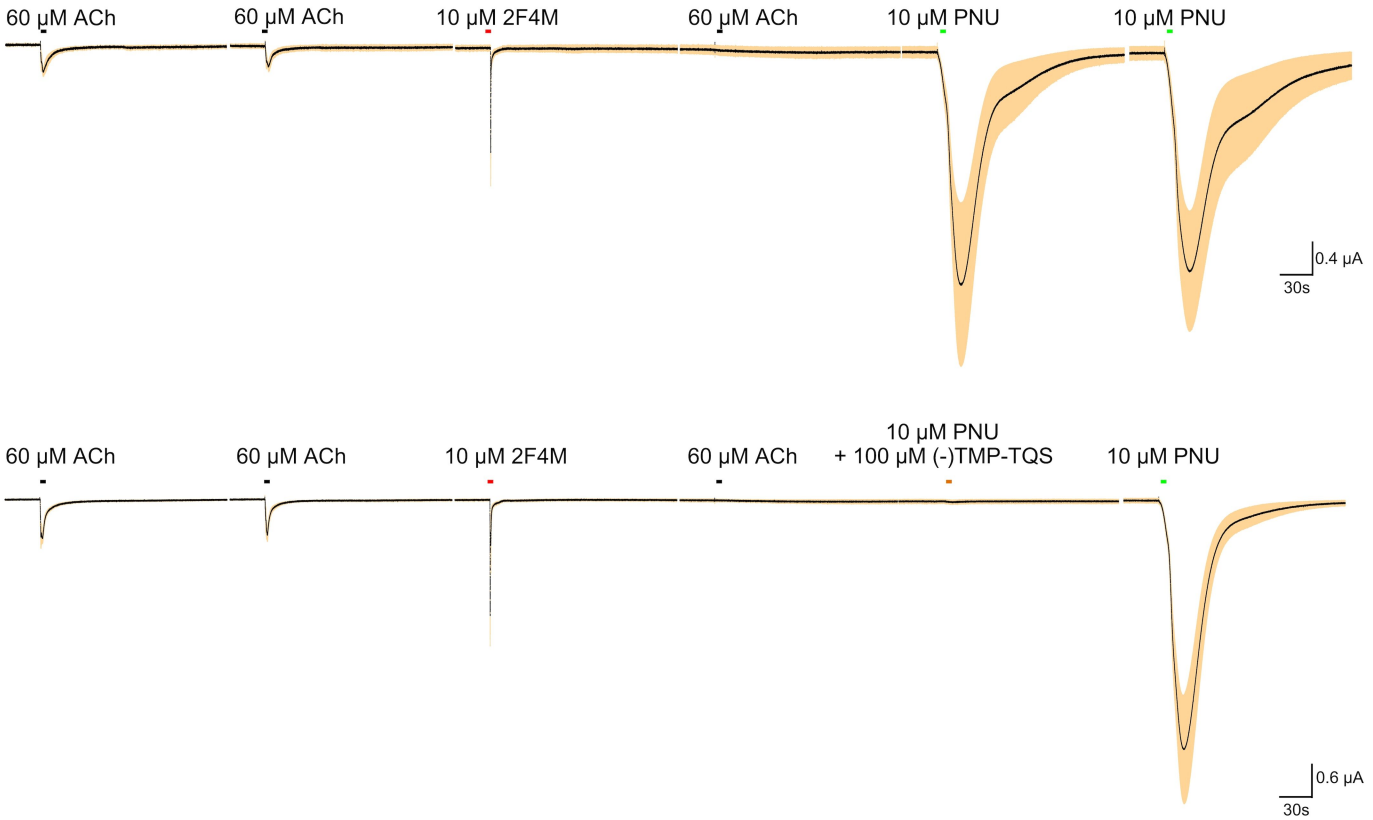

B

Cells given two applications of PNU-120596 alone

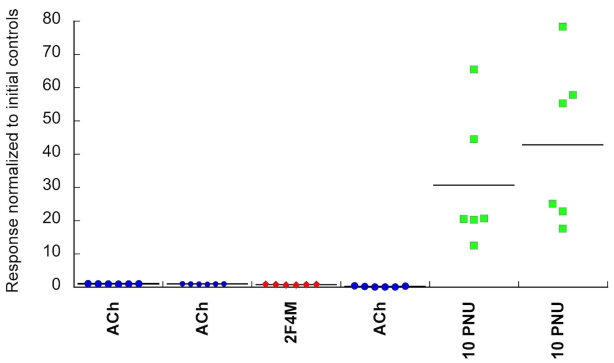

Cells given TMP-TQS with the first application of PNU-120596 alone

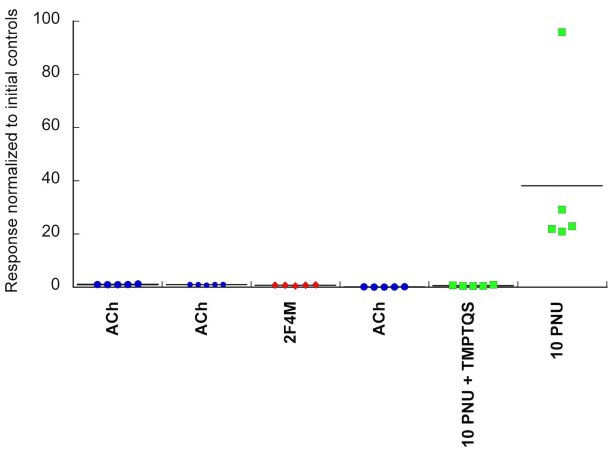

Figure 6

Effects of (-)TMP-TQS on α7 C190A responses to 2F4M

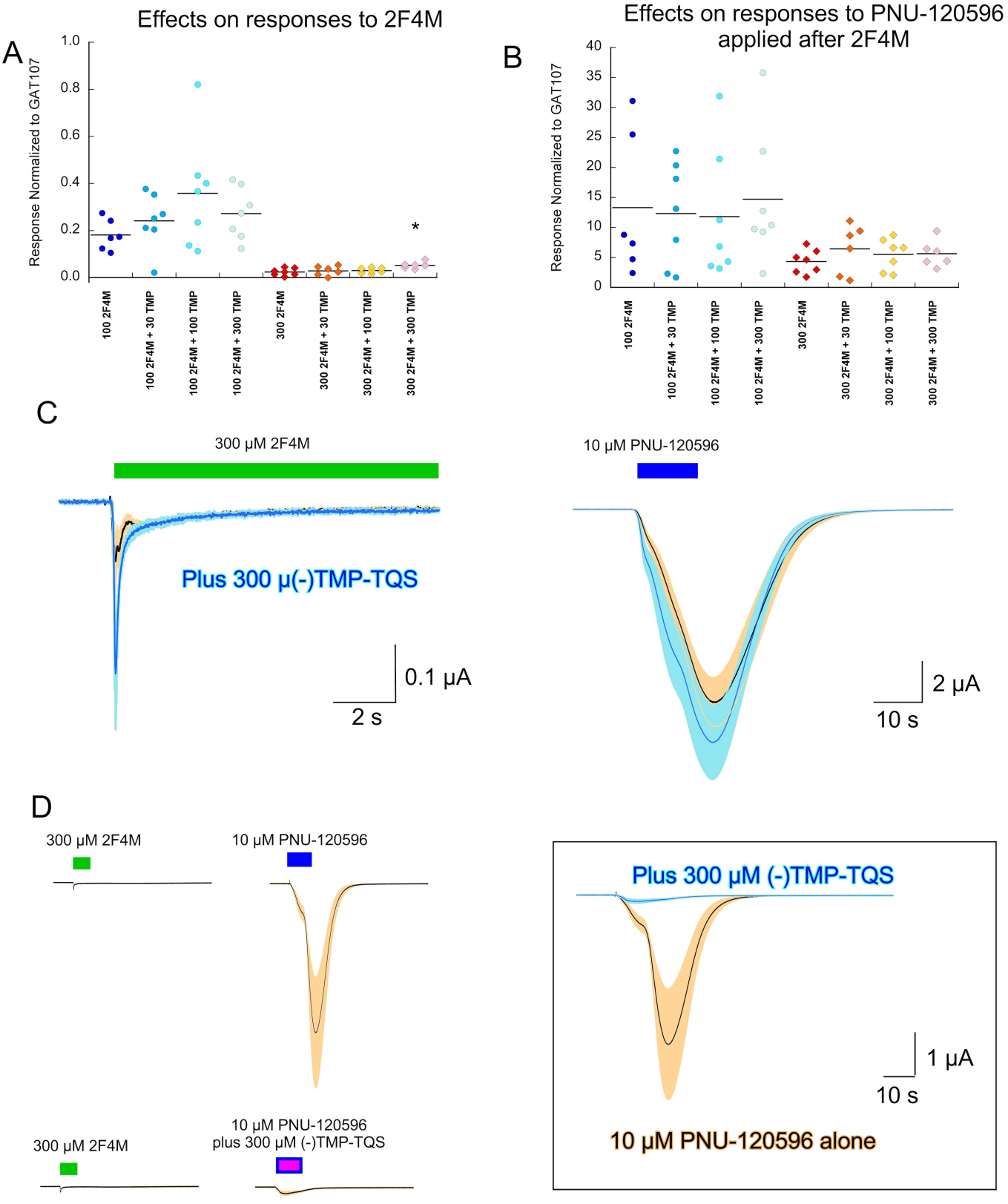

Figure 7

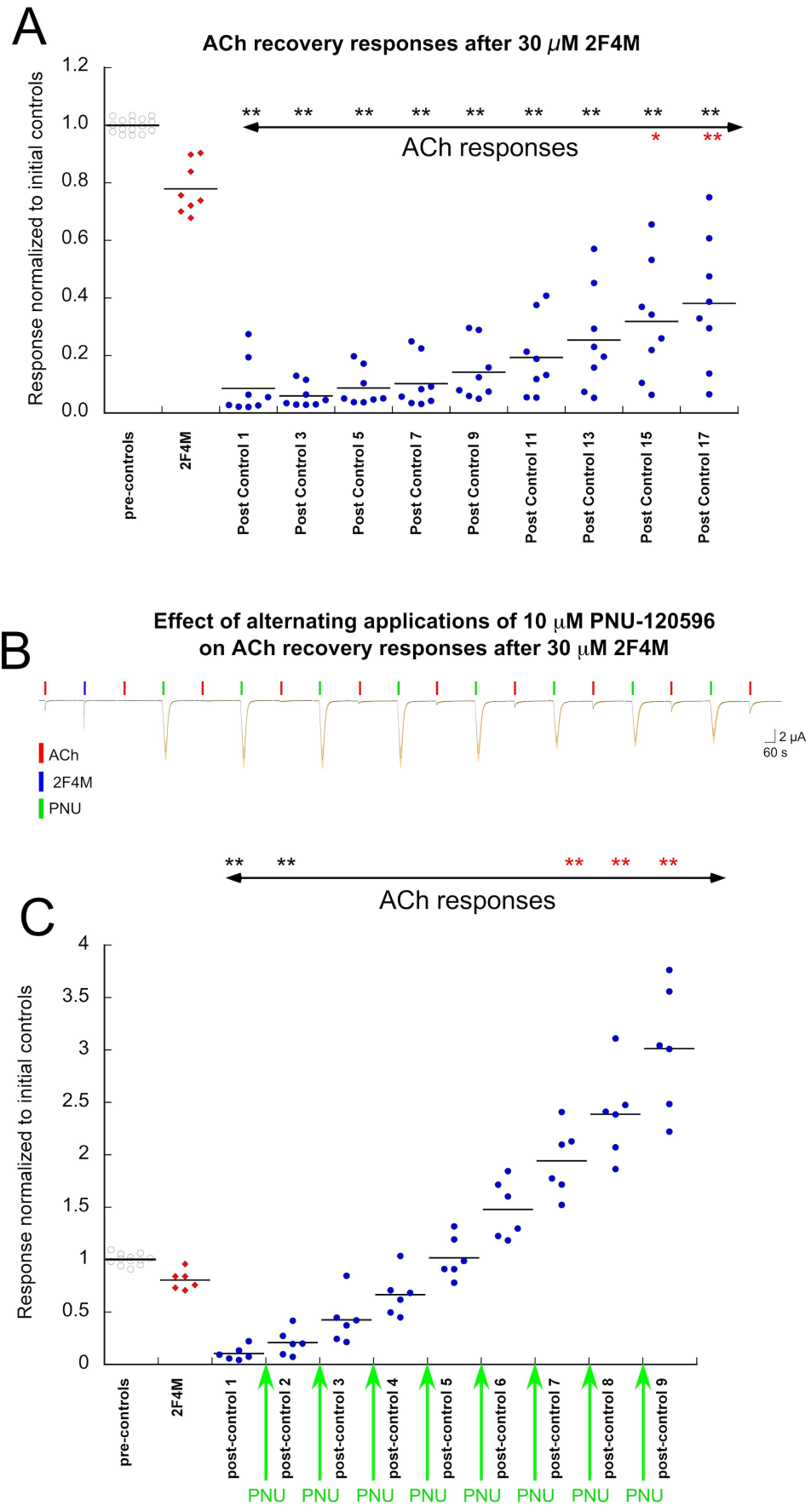
A
ACh recovery responses after 30 μM 2F4M
Response normalized to initial controls
1.2
1.0
0.8
0.6
0.4
0.2
0.0
** ** ** ** ** ** ** ** **
ACh responses
* **
pre-controls
2F4M
Post Control 1
Post Control 3
Post Control 5
Post Control 7
Post Control 9
Post Control 11
Post Control 13
Post Control 15
Post Control 17
B
Effect of alternating applications of 10 μM PNU-120596
on ACh recovery responses after 30 μM 2F4M
ACh
2F4M
PNU
2 μA
60 s
** ** ** ** **
ACh responses
C
Response normalized to initial controls
4
3.5
3
2.5
2
1.5
1
0.5
0
pre-controls
2F4M
post-control 1
post-control 2
post-control 3
post-control 4
post-control 5
post-control 6
post-control 7
post-control 8
post-control 9
PNU PNU PNU PNU PNU PNU PNU PNU

Figure 8

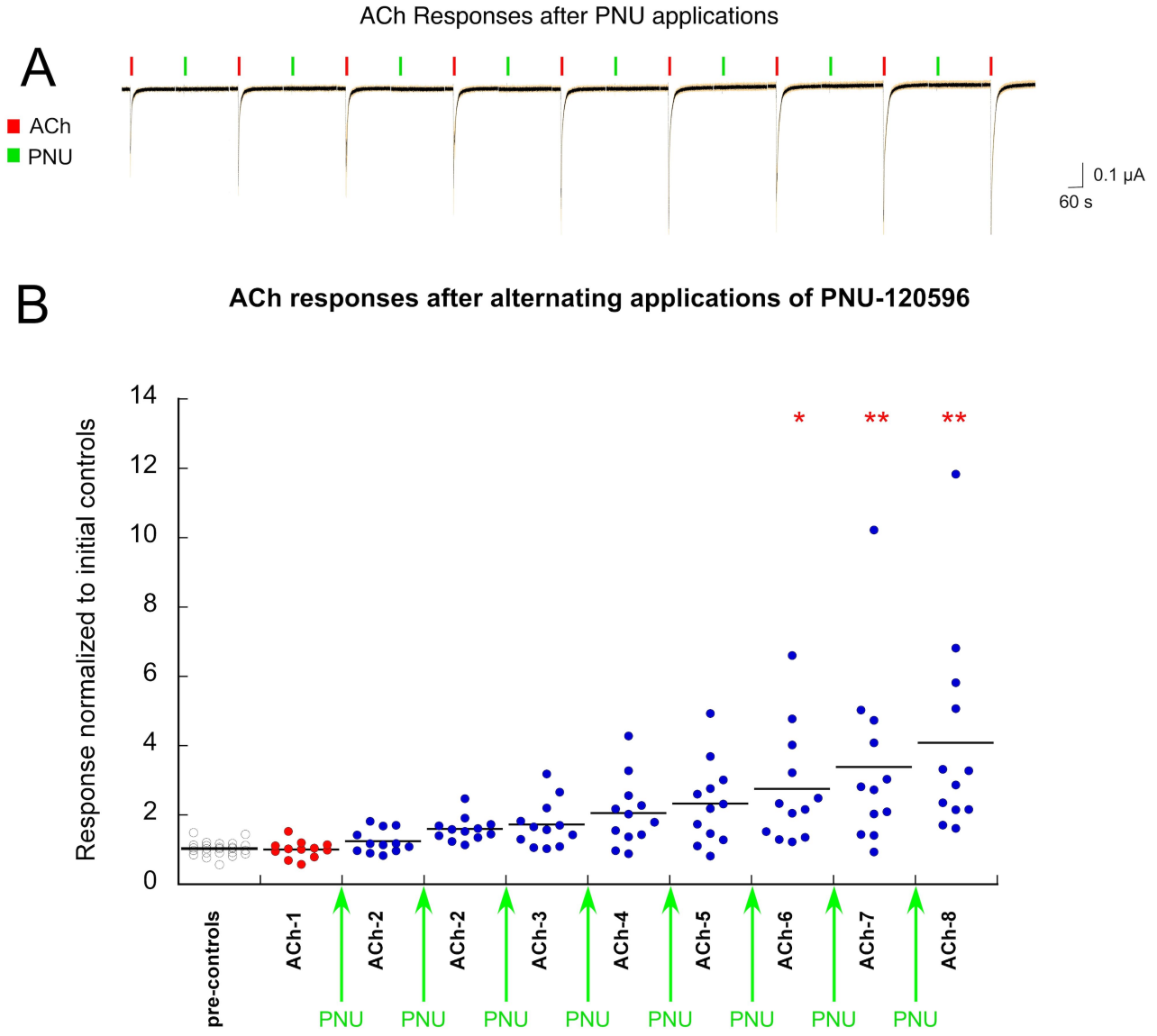
ACh Responses after PNU applications
A
ACh
PNU
0.1 µA
60 s
B
ACh responses after alternating applications of PNU-120596
Response normalized to initial controls
14
12
10
8
6
4
2
0
*
**
**
pre-controls
ACh-1
ACh-2
ACh-2
ACh-3
ACh-4
ACh-5
ACh-6
ACh-7
ACh-8
PNU
PNU
PNU
PNU
PNU
PNU
PNU
PNU

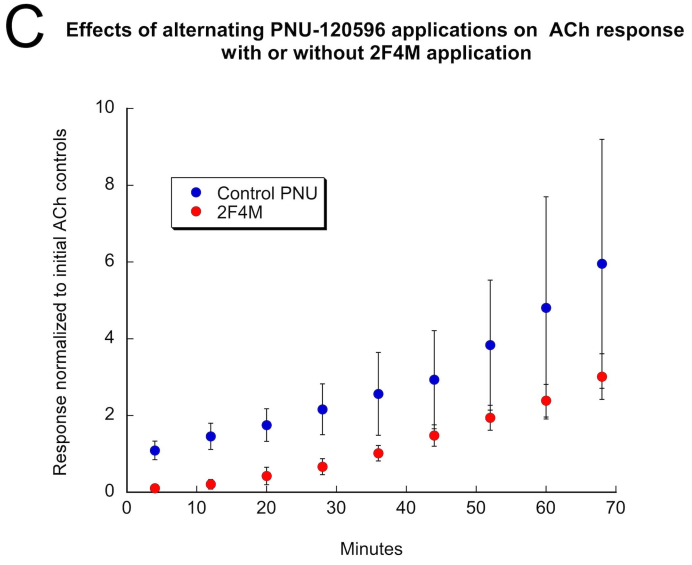
C
Effects of alternating PNU-120596 applications on ACh response with or without 2F4M application
Response normalized to initial ACh controls
Control PNU
2F4M
10
8
6
4
2
0
0
10
20
30
40
50
60
70
Minutes

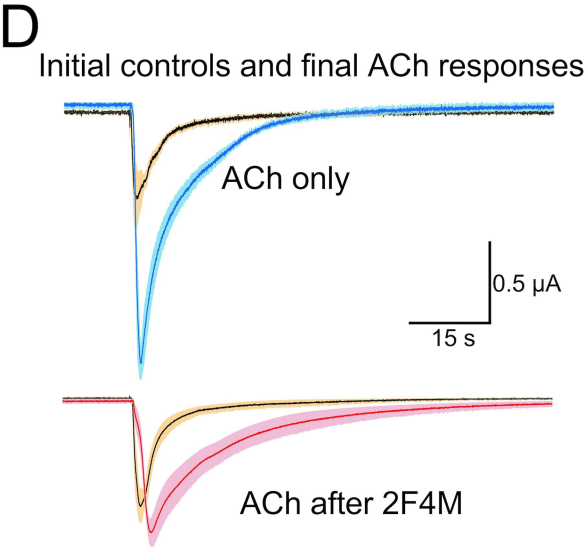
D
Initial controls and final ACh responses
ACh only
0.5 µA
15 s
ACh after 2F4M

Figure 9

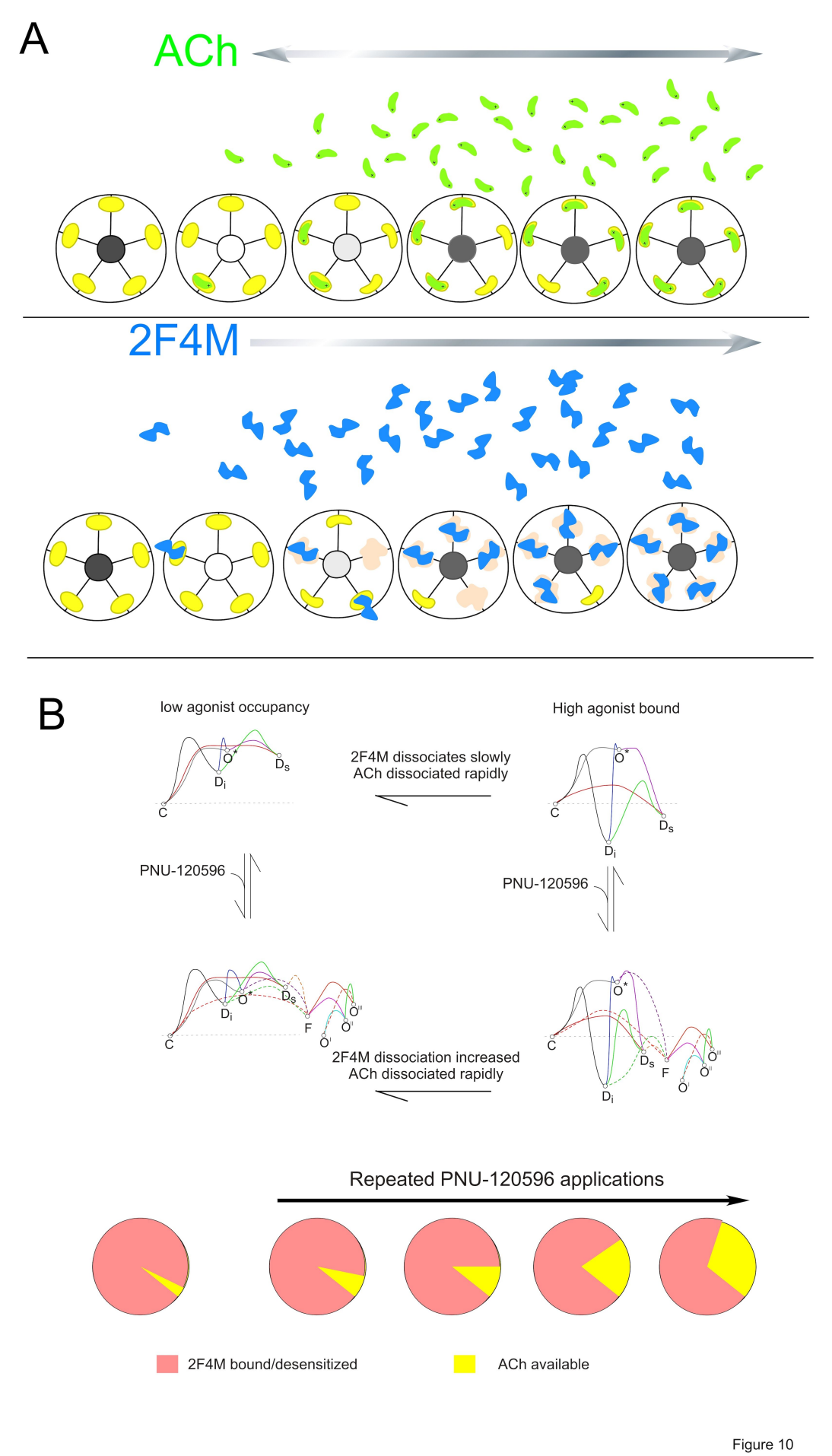
A
ACh
2F4M
B
low agonist occupancy
High agonist bound
2F4M dissociates slowly
ACh dissociated rapidly
PNU-120596
PNU-120596
2F4M dissociation increased
ACh dissociated rapidly
Repeated PNU-120596 applications
2F4M bound/desensitized
ACh available

Figure 10